



**Australian Government**  
**Bureau of Meteorology**

**The Centre for Australian Weather and Climate Research**  
A partnership between CSIRO and the Bureau of Meteorology



# Doppler weather radar in Australia

Susan J Rennie

**CAWCR Technical Report No. 055**

November 2012



[www.cawcr.gov.au](http://www.cawcr.gov.au)





# Doppler weather radar in Australia

Rennie, S.J.

*The Centre for Australian Weather and Climate Research  
- a partnership between CSIRO and the Bureau of Meteorology*

**CAWCR Technical Report No. 055**

November 2012

National Library of Australia Cataloguing-in-Publication entry : (pbk)

Author: Rennie, Susan J.

Title: Doppler weather radar in Australia / Susan Rennie.

ISBN: 9780643109483 (ebook : pdf)

Series: CAWCR technical report, no. 055.

Notes: Includes bibliographical references and index.

Subjects: Doppler radar.

Doppler tracking--Australia.

Weather radar networks--Australia.

Dewey Number: 534.3

Enquiries should be addressed to:

**Dr. Susan Rennie,**  
Centre for Australian Weather and Climate Research,  
GPO Box 1289,  
Melbourne, VIC, 3001  
AUSTRALIA  
email: s.rennie@bom.gov.au

## Copyright and Disclaimer

© 2012 CSIRO and the Bureau of Meteorology. To the extent permitted by law, all rights are reserved and no part of this publication covered by copyright may be reproduced or copied in any form or by any means except with the written permission of CSIRO and the Bureau of Meteorology.

CSIRO and the Bureau of Meteorology advise that the information contained in this publication comprises general statements based on scientific research. The reader is advised and needs to be aware that such information may be incomplete or unable to be used in any specific situation. No reliance or actions must therefore be made on that information without seeking prior expert professional, scientific and technical advice. To the extent permitted by law, CSIRO and the Bureau of Meteorology (including each of its employees and consultants) excludes all liability to any person for any consequences, including but not limited to all losses, damages, costs, expenses and any other compensation, arising directly or indirectly from using this publication (in part or in whole) and any information or material contained in it.

# Contents

- Summary.....1**
- 1. Introduction.....3**
- 2. Operational Doppler radars .....5**
  - 2.1 Radar fundamentals ..... 6
  - 2.2 On-site processing..... 9
- 3. Post-processing.....11**
  - 3.1 VAD profiles..... 11
  - 3.2 Dealiasing..... 12
  - 3.3 Data quality issues ..... 13
- 4. Clear air echo .....16**
  - 4.1 Insects ..... 16
    - 4.1.1 Comparison with model velocities..... 21
  - 4.2 Bird migration and dispersal ..... 23
  - 4.3 Fire observations ..... 25
  - 4.4 Chaff..... 25
- 5. Weather features observed with Doppler radar .....27**
- 6. Comparison against other observations .....31**
  - 6.1 Comparison with a wind profiler..... 31
  - 6.2 Comparison with Automatic Weather Stations..... 32
- 7. Assimilation of radial winds .....35**
- 8. Conclusion .....37**
- Acknowledgments .....38**
- References.....39**

## List of Figures

<b>Fig. 2.1</b> Locations of the Australian Doppler radars in 2012. S-band (■), C-band (●) and open circles to be installed in 2012. ....	5
<b>Fig. 2.2</b> Data types available from Doppler radars: uncorrected and corrected reflectivity, spectrum width and radial velocity. Example from Wollongong radar, 0.5° elevation scan at 0331 UTC 20/9/2011, containing precipitation, ground and sea clutter. Note the different colour scales. ....	10
<b>Fig. 3.1</b> a) Schematic of geometry of the radial wind for VAD calculation, ignoring curvature of the Earth. The radar beam follows the dashed line. b) VAD fit (red) to radial velocity data (black) from Terrey Hills, 0200 UTC 17/6/2010 at 1.3° elevation, 90 <sup>th</sup> range bin (22.5 km). ....	11
<b>Fig. 3.2</b> Data from Terrey Hills, 0200 UTC 17/6/2010 at 3.1° elevation. a) Raw radial velocity. b) Velocity dealiased with 4DD method. c) Velocity dealiased with Tabary method and no spatial dealiasing. ....	12
<b>Fig. 3.3</b> Reflectivity from 12 UTC 28/9/2010 at Brisbane (Mt Stapylton), for the 2 <sup>nd</sup> and 3 <sup>rd</sup> elevations. The clutter filtering was only effective on the lowest two elevations, producing the no-data areas (white) near the bottom of the left panel. The right panel instead shows reflectivity above zero. The height is calculated using equation 1. ....	14
<b>Fig. 3.4</b> Velocity as for Fig. 3.3. The clutter in the right panel manifests as near-zero velocity at low altitude. ....	14
<b>Fig. 3.5</b> VAD speed for lowest three elevations from 12 UTC 28/9/2010 at Brisbane (Mt Stapylton). The near-ground speed is lower for the 1.3° elevation with ground clutter. ....	15
<b>Fig. 4.1</b> Locust migration (unidentified species) in south-east Queensland and northern NSW in October 2010. The asymmetric reflectivity at Warrego denotes a distinct patch of locusts that migrated southwestward. Around Namoi the insects are more uniformly distributed. (Data holes due to ground clutter.) ....	17
<b>Fig. 4.2</b> Diurnal migration on the afternoon of 30/12/2010, at Yarrowonga, featuring insects aggregated by convergence lines around convective cells. ....	18
<b>Fig. 4.3</b> Schematic showing that insects present a larger target to the radar when illuminated side-on than head-on. ....	19
<b>Fig. 4.4</b> Example of common orientation in an early morning migration. a) Velocity of insects (blue towards radar). b) Reflectivity showing dumbbell with lobes to east and west of radar. c) Vertical profiles of the direction of orientation, direction of travel and crab angle (difference). Thick lines are volume-averaged, thin lines are for the 0.9° scan. Directions are given in degrees clockwise from north. ....	20
<b>Fig. 4.5</b> Comparison of clear air VADs with ACCESS-A model profile values (observation – background) of speed and direction. Data are coloured according to time of day in hours (UTC). Each data point represents a date-time and height. ....	21
<b>Fig. 4.6</b> Histogram of speed differences (left) and direction differences (right) (observation – background). The direction outliers have been excluded. Cumulative counts are from 22 instances and all available heights, as per Fig. 4.5. ....	22
<b>Fig. 4.7</b> Schematic of velocity vectors used for Table 4.1, where the Observed vector remains constant, and the length of insect air speed varies. ....	23
<b>Fig. 4.8</b> Dawn bird dispersal, at 0432 EST, 6/1/2011 at Yarrowonga. The points of high reflectivity indicate birds taking off and travelling south-southwestward. ....	24
<b>Fig. 4.9</b> Radial velocity at 0.5° elevation marking the bird migration across Port Phillip Bay in the afternoon at 1524 EST 15/9/2011, observed from the Melbourne radar. The radar location is marked by ♦; the bird migration is enclosed with the	

dashed box. The migration appears as a line of red velocity value as the birds travel south-southeastward. ....	24
<b>Fig. 4.10 Velocity from 2009 Black Saturday bushfires, 2/7/2009. At 0300 UTC there are two main fires, though one is obscured by clear air. At 0900 UTC, around sunset so minimal clear air, smoke from the bushfire complex is visible. There are also some scattered showers. ....</b>	<b>25</b>
<b>Fig. 4.11 Ground and sea clutter and chaff viewed with Wollongong radar (0.5° elevation scan) on 17/10/2011 at 0500 UTC. ....</b>	<b>26</b>
<b>Fig. 5.1 Velocity (left) and reflectivity (right) scans taken by the Yarrawonga radar from 1412 UTC 24/11/2010. Rain approaching from the west is preceded by a boundary that formed a wave train propagating west to east. Three lines are visible in the reflectivity. ....</b>	<b>27</b>
<b>Fig. 5.2 Velocity and reflectivity scans at 0.9° elevation, from the Melbourne radar. a) 0236 UTC 21/1/2011. A cool change moving in from the west is closely followed by a sea breeze passage from the south. b) 0348 UTC 21/1/2011. The front and sea breeze have merged north of Port Phillip Bay, but a second sea breeze front has developed to the east, from the Western Port Bay inlet to the east of Port Phillip Bay. ....</b>	<b>28</b>
<b>Fig. 5.3 Tornado passage during a storm passing south of Adelaide. Scans are 0.5° elevation from Buckland Park radar at 0401 and 0411 UTC 11/7/2009. The Buckland Park radar is just north of the upper axis limit. The tornado is circled. It is inferred by the dipole in the velocity field. ....</b>	<b>29</b>
<b>Fig. 5.4 Velocity and reflectivity from TC Carlos, Darwin (Gunn Pt research radar) at 2200 UTC 15/2/2011. ....</b>	<b>30</b>
<b>Fig. 6.1 Comparison of Yarrawonga VAD with subsampled 1 minute AWS wind observations. Speed (left) and Direction (right) are shown. VAD heights are relative to antenna height and represent the middle of the 100 m height bin. AWS stations are Yarrawonga, Shepparton AP, Rutherglen and Wangaratta Aero. Time is in UTC. ....</b>	<b>33</b>
<b>Fig. 6.2 Comparison of Terrey Hills VAD with subsampled 1 minute AWS wind observations. Speed (left) and Direction (right) are shown. VAD heights are relative to antenna height and represent the middle of the 100 m height bin. The AWS stations are Sydney AP, Kurnell, Terrey Hills and Richmond RAAF. Time is in UTC. ....</b>	<b>33</b>
<b>Fig. 7.1 Potential radar coverage to 120 km (shaded), and approximate city domains for the 1.5 km ACCESS high resolution model. ....</b>	<b>36</b>

## List of Tables

<b>Table 2.1 Specifications of the Australian Doppler radars in 2012.</b> .....	6
<b>Table 2.2 Height above ground level and width for a beam with an elevation angle of 2.5°</b> .....	8
<b>Table 4.1 True wind speed assuming insects have air velocity in the direction of their orientation, and at various speeds, assuming the observed velocity (ground speed) is 12 m s<sup>-1</sup> and 30°.</b> .....	23
<b>Table 6.1 Vector correlation coefficient (<math>r^2</math>) (Crosby <i>et al.</i>, 1993) between VAD and WP data separated by WP speed, and number of samples (n). (Reproduced from Rennie <i>et al</i> (2011b))</b> .....	31

## SUMMARY

As part of recent programmes<sup>1</sup> to update its weather radar network, the Australian Bureau of Meteorology has implemented Doppler capability at some radar sites. The new Doppler radars provide high spatial and temporal resolution observations of the radial velocity of radar targets. Radial velocity has a range of applications, including enhancements to radar data processing and quality control, and high resolution visualisation of the velocity associated with weather features. The primary use of Doppler information is to estimate the wind velocity using precipitation echo. This can be enhanced by the use of clear air echo, primarily from insects, when there is no precipitation present. For example, insect echo can show sea breeze convergence lines. Other non-precipitation echo reveals bushfire smoke propagation and occasionally bird migration and dispersal.

There are a range of issues affecting data quality that must be considered when using radial velocity. Some issues are associated with the instrument and how it makes measurements, for example the radar beam's width and propagation. Other issues result from the characteristics of the echo source, i.e. the backscatter targets, particularly the targets' own velocity. A major source of error in radar data is echo from the ground or sea, from which contamination can cause highly erroneous velocity estimates. These issues, and how they impact on radar applications, are discussed in this report.

For numerical weather prediction (NWP) applications like data assimilation it is necessary to ensure that velocity estimates are representative of the wind field. Comparisons with wind profiler and surface observations showed good agreement; the differences between these observation types conformed to those predicted by knowledge of the instrument biases and measurement method. Comparisons so far have shown no significant difference between clear air (insect) and precipitation-derived wind observations: these showed similar uncertainties and biases. Although the types of insects that are probably detected by the radar are capable of flight at several  $\text{m s}^{-1}$ , and showed indications of controlling their migration direction, comparison with model wind estimates did not indicate a bias greater than the expected uncertainty in velocity. Therefore it should be possible to assimilate radial velocity from insects as well as precipitation.

High-resolution NWP is important for short-range severe weather forecasts. Assimilation of high-resolution observations will improve the initial conditions for such forecasts. This will bridge the gap between nowcasting and forecasting by reducing the model spin-up time for the production of a skilful forecast. Radar data are ideal for assimilation in high-resolution NWP models because of their temporal and spatial coverage. The various sources of error in radial velocity observations, particularly measurement uncertainties, will dictate how observations are used for data assimilation.

---

<sup>1</sup> Radar Network and Doppler Services Upgrade Project (RNDSUP) and Strategic Radar Enhancement Project (SREP).

This report aims to summarise Australia's upgraded operational weather radar network's capabilities with regard to Doppler radar. Topics covered include the range of weather and non-weather observations drawn from the radars, and some of the applications of these observations. The report provides a general overview of Doppler radar data, from collection across the network, through on-site and off-site processing and quality control, to practical applications of the data in weather forecasting.

# 1. INTRODUCTION

Australia's weather radar network, operated by the Bureau of Meteorology (BoM), consists of around 60 radars and covers most coastal and some inland regions of the continent. The network design features radars located in highly populated areas and along the coastlines, particularly the northern coastline where tropical cyclones threaten during the wet season (austral summer). Some radars are also used part-time for wind-finding. Australia is very large and sparsely populated, so a radar network that provides total coverage is not practical. The communication network required to transmit the data to a central location also influences the network design, as well as associated hardware and software choices.

During upgrades to the network starting in 2003 as part of the Radar Network and Doppler Services Upgrade Project (RNDSUP), enhanced Doppler capabilities were implemented at six radar locations. The upgraded radars are dual-polarisation ready (Jarrott *et al.* 2007). Dual polarisation would provide substantial improvements in options for quality control and quantitative precipitation estimation (QPE), and so future upgrades should eventually include using the dual-polarisation capability. In 2010, the Strategic Radar Enhancement Project (SREP) was initiated, with funding for four years. SREP will see the installation or upgrade of four additional Doppler radars (Hobart (TAS), Wollongong (NSW), Mount Isa (QLD) and Waruwi (NT)).

The new radars are intended to help improve qualitative analysis and nowcasting, particularly for severe thunderstorms and flash flooding. When upgrading some of the radars to provide Doppler data, priority was given to capital cities (high population density) and areas prone to severe weather, as well as closing gaps in the existing network. No Doppler observations are collected from radars located in Western Australia or central Australia, although three are located in inland areas of the eastern states and a fourth to be installed near the QLD/NT border.

Besides the radar network upgrade, SREP aims to increase the use of radar data in forecasting through data assimilation into high-resolution mesoscale models. Data assimilation improves the initial conditions of the model run and so reduces the spin-up time, providing a skilful forecast sooner. This will help close the gap between nowcasting and forecasting. To better enable quantitative applications, the data processing and quality control procedures will be enhanced, to provide higher-quality reflectivity data for QPE as well as more accurate radial velocity measurements. It will also be possible to make use of clear air echo, to expand the observation coverage, but whose benefit must still be established.

Doppler provides various advantages over reflectivity-only radar. Firstly, it can provide information about the wind field by its ability to measure the radial component of the movement of hydrometeors. The spatial resolution and coverage of these wind observations are unmatched by other instrument types. Secondly, it enables enhanced clutter detection and removal, including detection of non-permanent ground echoes. The ability to filter clutter in real time is a substantial advantage to data quality procedures.

Many countries' radar networks now include Doppler capability for some, if not all radars. The USA has a network of over 150 Doppler radars that are being upgraded to dual-polarization capability at present (Weber *et al.*, 2007). The UK's network including seven Doppler radars (Met Office, 2009) has been expanded (Met Office, pers. comm. 6 August 2012) and is

upgrading the network to Doppler with dual-polarisation (Met Office, 2012). France has almost total Doppler coverage including some dual and triple Doppler coverage (Montmerle and Faccani, 2009). Many other European countries have at least one Doppler radar, and some combine efforts (e.g. NORDRAD/BALTRAD, Michelson *et al.*, 2010). Morocco, Lithuania, Romania and other European countries have established Doppler radar networks (Huuskonen *et al.*, 2010). In Europe, the Operational Programme for the Exchange of weather RADar information (OPERA) involves many European countries, and aims to improve radar data quality and use amongst them. OPERA proposes to facilitate the exchange of expertise in weather radar, and make the processing and storage of radar data more uniform (Huuskonen *et al.*, 2010). From this, radar data can be interchanged freely among participating countries and combined in weather forecasting applications. The latest stage ‘Odyssey’ produces a 2 km gridded composite radar data from up to 120 radars for dissemination to parties (Dupuy *et al.*, 2011).

Until recent years, there had been little quantitative use of radar data in operational numerical weather prediction (NWP). Radar data were used directly by forecasters, or for nowcasting (Mueller *et al.*, 2003; Bowler *et al.*, 2004). With increases in computational power, NWP can now utilise models with resolution in the order of kilometres (e.g. Dance, 2004). This resolution is comparable to that of radar data, so it becomes possible to assimilate radar observations. For example, the UK Met Office now assimilates radial winds using 3D-Var into their 1.5 km horizontal-resolution model (Hawkness-Smith *et al.*, 2011). They are also intending to use wind measurements from insect echoes, which will provide coverage during fine periods, and be of particular use during convective development (Rennie *et al.*, 2011a).

For high-resolution NWP in Australia, radar data coverage exceeds that of any other observation type, within the radar domain and when there is signal. Therefore radar can become a predominant source of observations. Australia also has abundant clear air echo from insects during warmer months, which should be carefully assessed as a source of observations, but has the potential to greatly increase spatial and temporal coverage.

This report describes the potential of these instruments in Australian weather forecasting. Section 2 describes the instruments and how they work, as well as the signal processing. Section 3 details the post-processing for Doppler data. All sources of clear air echo are discussed in Section 4. Section 5 describes various weather features that can be observed with Doppler radar. In Section 6 comparisons are made with other atmospheric observations from various instruments including surface observations and wind profiles. Section 7 provides recommendations for the preparation of radial wind observations for ingestion into a data assimilation system.

## 2. OPERATIONAL DOPPLER RADARS

The Australian weather radar network consists of a mixture of S-band and C-band radars. There are also dual-polarised research radars near Darwin and Brisbane, and additional radars located at airports that may be used as backup during scheduled maintenance. This report focuses only on the weather radar network.

The Doppler radars' specifications are listed in Table 2.1, and locations are shown in Fig. 2.1. All but five Doppler radars are S-band; the exceptions are Darwin, Kurnell, Mt Koonya, Yarrowonga and the forthcoming Arafura which are C-band. S-band radars are usually preferred for tropical regions where it is desired to view precipitation at long ranges, since attenuation through heavy precipitation is less.

The BoM adopted a scan strategy for its radars that is appropriate for the severe weather types seen in Australia. All radars use plan position indicator (PPI) scanning, which involves scanning a full circle at a constant elevation angle relative to the ground. To monitor deep convection, and conduct quantitative precipitation estimation (QPE), the radars operate with 6 or 10 minute cycles, allow clear air detection, and have a minimal 'cone of silence' (Gunn *et al.*, 2007), i.e. the unobserved region right above the radar. The radars typically scan over 14 elevations: 0.5°, 0.9°, 1.3°, 1.8°, 2.4°, 3.1°, 4.2°, 5.6°, 7.4°, 10°, 13.3°, 17.9°, 23.9° and 32°.



Fig. 2.1 Locations of the Australian Doppler radars in 2012. S-band (■), C-band (●) and open circles to be installed in 2012.

**Table 2.1 Specifications of the Australian Doppler radars in 2012.**

Radar (Location)	Location	Height	Band	Angle res. (beam width)	Range res. (m)	Nyquist vel. (m s <sup>-1</sup> )	Range (km)
Adelaide (Buckland Park)	138.469 -34.617	30	S	1°	250	39.9	150
Melbourne (Laverton)	144.752 -37.852	14	S	1°	250	52.2	150
Yarrawonga (NE Vic)	146.03 -36.03	146	C	1°	250	26.6	150
Wollongong (Appin)	150.874 -34.264	449	S	1° (2°)	500	31.2	300
Kurnell (south Sydney)	151.226 - 34.0418	64	C	1°	250	26.6	150
Sydney (Terrey Hills)	151.21 -33.701	195	S	1°	250	26.1	300
Namoi (Blackjack Mt)	150.191 -31.024	699	S	1° (2°)	500	39.0	200
Brisbane (Mt Stapylton)	153.24 -27.718	175	S	1°	250	52.1	150
Emerald (central Qld)	148.239 -23.549	211	S	1° (2°)	500	39.0	200
Gympie (Mt Kanigan)	152.577 - 25.9574	375	S	1°	500	19.5	200
Darwin (Berrimah)	130.925 -12.457	62	C	1°	250	26.5	150
Koonya (Hobart)	147.806 -43.112	511	C	1°	250	26.7	150
Mount Isa	forth- coming		S	(2°)			
Arafura	forth- coming		C	1°			

## 2.1 Radar fundamentals

This section gives a brief overview of radar operation, and some problems that are inherent in radial velocity measurement. The focus is on theory relevant to later analyses in this report. More detail can be found in a radar text book such as Doviak and Zrnić (1993), or the relevant radar manuals and documentation.

Weather radars transmit an electromagnetic beam in the form of a sequence of pulses, and alternate transmission and reception using the same antenna. The beam is reflected off any targets along its path and a small fraction of the scattered energy is directed back to the antenna. The strength of the returned signal is a function of the amount and type of backscatter targets within the volume that a pulse illuminates.

The distance of the target from the radar is indicated by the return delay of the signal. The returned signal is segmented into range bins. Beyond a certain point, the returned signal will overlap with the next pulses and so become ambiguous. The unambiguous range is the distance at which the location of the scattering radar target can be unambiguously assigned. Second-trip echoes are echoes that return after then next pulse has been transmitted. Information from these may be retrieved by identifying echoes from the previous pulse. This technique (known as phase-coding) is currently used only for the Terrey Hills and Wollongong radars, doubling the effective range.

As the radar beam propagates through the atmosphere it is refracted by the vertical gradients in atmospheric density. This in combination with the curvature of the Earth means that the computation of the actual height of the beam above the Earth is not trivial. The refractive effect of the atmosphere is greater at low beam elevations. The true path of the beam can only be determined with knowledge of the atmospheric state, which is not usually available. The atmospheric state can be estimated using model data or atmospheric observed profiles from representative soundings, for example. However, it is a common practice to approximate the effect of atmospheric refraction.

One common approximation of the beam propagation (from Doviak and Zrnić (1993) and Ge *et al.* (2010)), commonly referred to as the 4/3 Earth method, is shown here:

Let  $R_{eff} = \frac{4}{3}R$  be the effective radius of the Earth. The height  $h$  of the radar beam above the surface at range  $r$  from the radar and at radar beam elevation angle  $\alpha$  is

$$h = \sqrt{r^2 + R_{eff}^2 + 2rR_{eff} \sin \alpha} - R_{eff}. \quad (1)$$

The beam elevation  $\theta$  relative to a local tangent to the surface at some range  $r$  from the radar is the angle  $\alpha + \varepsilon$  where

$$\varepsilon = \tan^{-1} \left( \frac{r \cos \alpha}{r \sin \alpha + R_{eff}} \right). \quad (2)$$

Even with beam propagation modelling, it is possible that uncertainties in this will induce a substantial error in vertical position at long ranges (Fabry, 2010). However, if it is possible to predict extreme cases when ducting occurs, that is to say that the beam is refracted back toward the surface and produces anomalous propagation (anaprop) echo, then at such times data may be discounted. Table 2.2 provides the height and beam width (on the vertical axis) of a 2.5° elevation beam with 1° beam width. At long ranges, the uncertainty in beam height may become large, especially at low elevations. Note also that as the beam quickly widens to more than 1 km, the vertical target distribution within the beam may be strongly non-uniform. The returned signal will be weighted by where the target signal is strongest.

**Table 2.2 Height above ground level and width for a beam with an elevation angle of 2.5°**

Range km	25	50	75	100	125	150
Beam width m	436	872	1307	1743	2178	2613
Height m	1127	2328	3602	4949	6340	7864

Doppler radar measures the frequency shift of the returned signal as a result of movement of the backscatter targets along the beam's trajectory. Only radial movement relative to the radar location is detected. The radial velocity is a component of the three dimensional velocity of a target, given by

$$V_R = u \sin \phi \cos \theta + v \cos \phi \sin \theta + w \sin \theta, \quad (3)$$

where  $\theta$  is the local elevation ( $\alpha + \varepsilon$ ),  $\phi$  is the azimuth, and  $u$ ,  $v$  and  $w$  are the Cartesian components of the velocity oriented eastward, northward and vertically with respect to the surface of the Earth. The full, three-dimensional velocity can not be retrieved without further information.

If the frequency shift is greater than or equal to  $180^\circ$ , it becomes ambiguous and so the velocity is folded or aliased. The maximum unambiguous velocity is known as the Nyquist velocity  $V_N$ , and may be determined by the following equation:

$$V_N = \frac{\lambda}{4} PRF$$

For example, with a Nyquist velocity of  $10 \text{ m s}^{-1}$  a radial velocity of  $13 \text{ m s}^{-1}$  will be observed as  $-7 \text{ m s}^{-1}$ : a difference of twice the Nyquist velocity. The Nyquist velocity can be increased by increasing the PRF, by using a radar with a longer wavelength, or by employing specialised scanning strategies such as the use of a dual pulse repetition frequency (PRF). The alternating of two different pulse frequencies allows overlapping signal returns to be disentangled. In this case the unambiguous velocity is increased to become a multiple of the two Nyquist velocities from each pulse repetition frequency.

The radar samples a volume encompassed by the beam width and the ranges at which the radar's signal processing system partitions the returned echo (by time of arrival), as per Table 2.1. Within this volume there may be a large number of targets moving with different velocities, e.g. due to turbulence or shear. The received signal therefore will have a spectrum of frequency shifts. Since the distribution of radar targets is unlikely to be uniform throughout the volume, and the beam shape has greatest power density at the centre of the beam, the velocity spectrum will be a convolution of these. The 'measured' radial velocity is the mean of the velocity spectrum, so it will be weighted to where the strongest backscattered signal has originated from. For rainfall, the signal response usually increases towards the lower part of the sample volume (larger target sizes), so the velocity is biased towards that part of the sample volume that is nearer the ground.

## 2.2 On-site processing

Details of on-site processing, i.e. that processing done at the radar site before any data are transmitted elsewhere, can be found in the Weather Watch Radar Software Documentation (Australian Bureau of Meteorology). The main points are summarised here.

The signal received by the antenna is captured as in-phase ( $I$ ) and quadrature ( $Q$ ) components.  $I$  and  $Q$  are orthogonal components of the raw signal. This raw signal can undergo a variety of processing before the resulting data are transmitted off-site. Typically the first few moments are calculated, i.e. reflectivity, velocity and spectrum width. The raw signal can also be used for quality control such as clutter filtering. Thus a substantial amount of on-site processing may be conducted before the data are transmitted. For Australian Doppler radars the software provided by the radar manufacturer is used for quality control processing.

Spectral filtering is used to reduce ground clutter. The signal is converted from the time domain to the frequency domain using a Discrete Fourier Transform (DFT), and the result is converted to a power spectrum. The clutter removal replaces points about 0 Hz with an estimate of the power interpolated from adjacent points. It assumes that the spectrum width of precipitation is much greater than that of clutter. Typically the maximum power reduction possible is 30–35 dB, so very strong clutter signals may persist. This filtering can also reduce power along the zero isodop, leading to a bias.

There are other published methods designed to identify clutter using the raw signal (e.g. Sugier *et al.*, 2002; Hubbert *et al.*, 2009a). These involve creating a parameter which represents the stationariness of the target. Such methods can be very effective. The Clutter Mitigation Decision algorithm which uses the Clutter Phase Alignment parameter (Hubbert *et al.*, 2009b) may be implemented by the Bureau in future.

To remove erroneous values, thresholding is also applied to corrected and uncorrected reflectivity, and velocity. Signals below some specified value (typically  $>2$  dB) above the radar noise floor are removed. Volumes with excessive clutter correction ( $>25$ – $30$  dB) are also removed. The Signal Quality Index (SQI) is calculated to remove noisy measurements. This is  $|R_1|/R_0$ , i.e. the power normalized modulus of the autocorrelation at lag one. An SQI value of 0 indicates white noise, and a value of 1 is a pure tone. A threshold for SQI may be applied, which is normally between 0.3 and 0.4. All threshold values are tuned for each radar.

After all processing is completed the data are written to a compressed format and transmitted off-site. The format used by the BoM is rapic (RADAR PICTure), which is a compressed format developed in-house. The Doppler radars all transmit the first two moments: reflectivity factor ( $Z$ ) and radial velocity ( $V$ ). Wollongong also transmits uncorrected reflectivity and spectrum width, for research purposes. Uncorrected reflectivity has not been corrected for attenuation, clutter filtering or thresholding. These four parameters are shown in Fig. 2.2. Note the ground clutter around the radar with very high uncorrected (and corrected) reflectivity, and zero velocity. Although clutter filtering was in place, it was not effective at all elevations. There is also sea clutter offshore, probably from side-lobe echoes, which appears to radiate from the radar location.

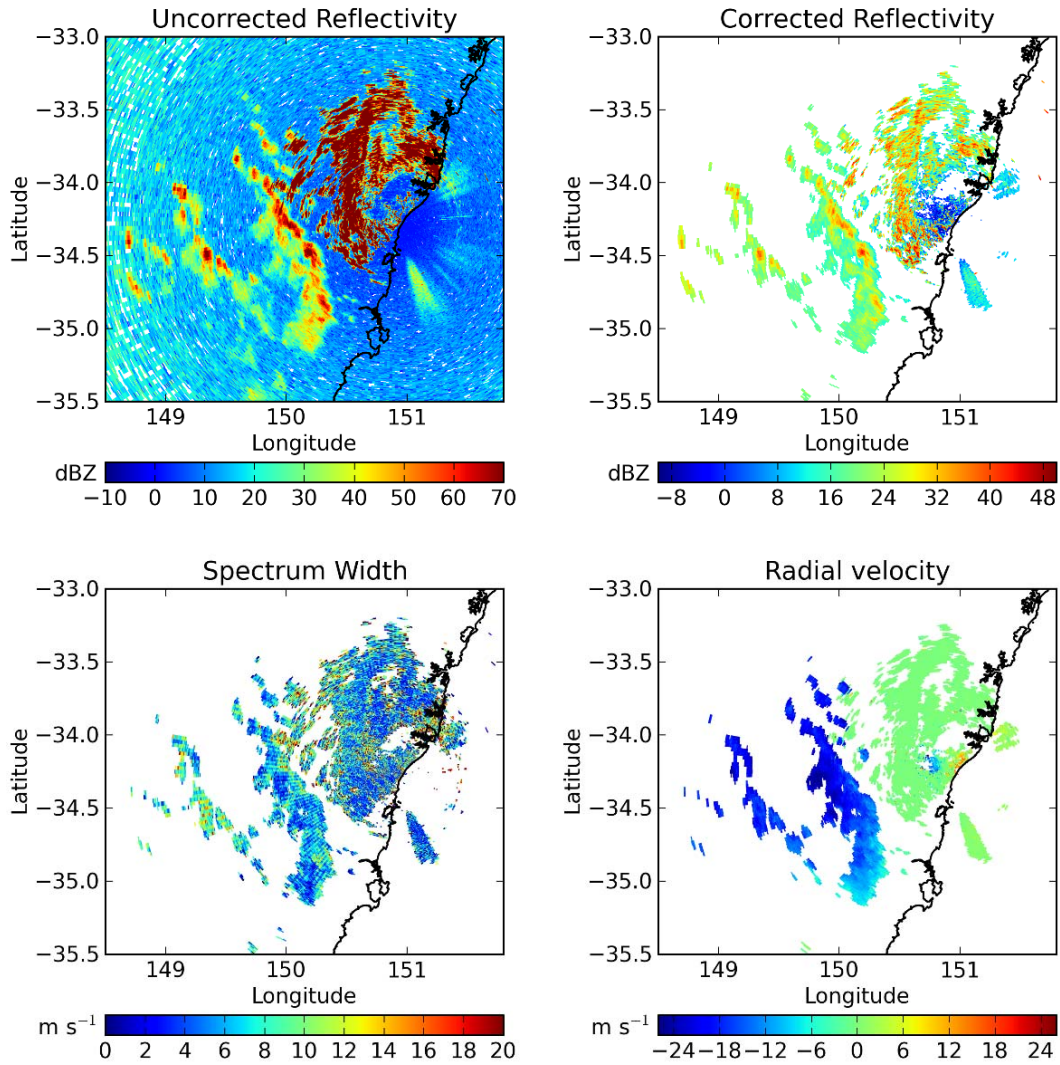


**Fig. 2.2** Data types available from Doppler radars: uncorrected and corrected reflectivity, spectrum width and radial velocity. Example from Wollongong radar, 0.5° elevation scan at 0331 UTC 20/9/2011, containing precipitation, ground and sea clutter. Note the different colour scales.

### 3. POST-PROCESSING

The data transmitted after the on-site processing may still have quality control issues to be addressed before the data are used for NWP. A range of non-weather echoes are likely to be present. Ground clutter can remain, particularly for radars near high terrain. Anaprop can result in further ground and sea clutter; in some areas strong inversions are often present to induce sea clutter. There will be biological echoes which need to be discriminated. Of these, insect echoes may be useful (see below) but echoes from birds or bats are not. There are non-biological echoes from chaff (metallic material typically released during air force exercises) and other random (speckle) echoes or interference signals e.g. from planes and ships. Finally, it is still possible to have folded velocity even with a Nyquist velocity up to  $30 \text{ m s}^{-1}$ .

#### 3.1 VAD profiles

The Velocity Azimuth Display (VAD) technique (Browning and Wexler, 1968; Andersson, 1992; Michelson *et al.*, 2000) is a means to create a vertical profile of horizontal wind from a radial wind scan. The output is a profile approximating the horizontal wind field above the radar location. The wind field is assumed to be linear. Some techniques can also estimate the vertical wind component from the convergence. The resultant data are analogous to a conventional wind profiler observation. Although there are no plans to use VADs in NWP, they can provide useful information to forecasters, and are also beneficial in processing and quality control. Furthermore, they can more easily be compared with other wind estimates, such as in Section 6. Therefore the method will be described here to help clarify subsequent sections.

The VAD method used here followed Michelson *et al.* (2000). For each individual scan, the data in each range ring (Fig. 3.1a) are used to create a single wind estimate at the equivalent height (as per equation 1). For this method a minimum number of diametrically opposite data pairs must exist. A least square's fit of a sinusoid is made (Fig. 3.1b) to the diametrically-opposite pairs, and the resultant phase and amplitude are used to determine the speed (corrected for beam elevation) and direction. A scan-averaged VAD is calculated by binning the VADs from all scans into height intervals of e.g. 100 m. This creates a smoother profile, with reduced uncertainty. It must be remembered that the radar beam illuminates a volume with dimensions greater than the height intervals of the VAD, so the profile is effectively smoothed and adjacent values are correlated.

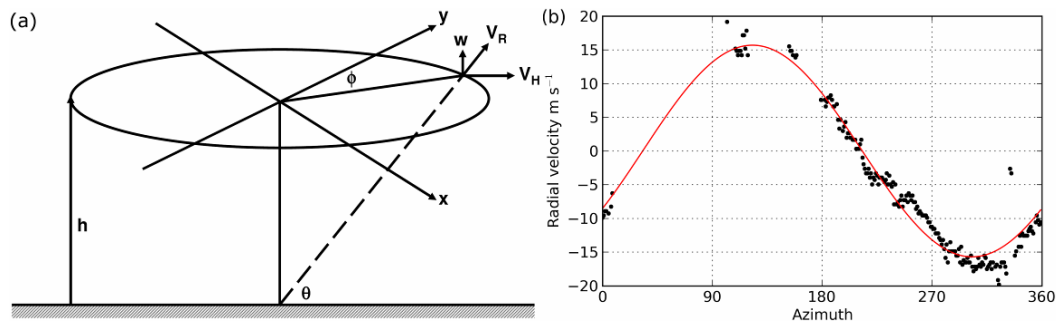


**Fig. 3.1 a)** Schematic of geometry of the radial wind for VAD calculation, ignoring curvature of the Earth. The radar beam follows the dashed line. **b)** VAD fit (red) to radial velocity data (black) from Terrey Hills, 0200 UTC 17/6/2010 at 1.3° elevation, 90<sup>th</sup> range bin (22.5 km).

## 3.2 Dealiasing

Aliasing is a sporadic problem, occurring only when the wind speed exceeds the Nyquist velocity. It is more frequently seen for radars with lower Nyquist velocity, such as Yarrowonga, Terrey Hills and Gympie. Dealiasing aims to correct the velocity by adding or subtracting twice the Nyquist interval. Uncorrected or wrongly corrected values will have a very large error.

There are various dealiasing methods in the literature. Two methods were tested in consideration for eventual inclusion in operational software. The first adopts the algorithms of James and Houze (2001), which uses a 4D comparison, and also compares with wind profiler data if available. This is possible for very few radars. The 4D dealiasing (4DD) method is fairly accurate and fast if used for dealiasing consecutive scans in real time. The idea of the method is to first compare each scan with the scan directly above it, and the corresponding elevation scan from the previous volume. This comparison comprises the time and height dimensions. The second stage is to do a spatial comparison, incorporating the radial and azimuthal dimensions. The spatial comparison involves a sweep along each radial, starting around the zero isodop, to produce a consistent, smooth velocity field. A second spatial comparison handles the remaining undealiased pixels, and examines a window around them to determine the correct velocity.

The second is based on Tabary *et al.* (2001) and uses the azimuthal gradient of  $V_R$  to estimate the true velocity. The Tabary method can be slow because it uses a minimization algorithm. However, it is able to be applied to a single volume without any corroborating data. This was useful for research purposes, including for initiating the 4D method by dealiasing the previous volume.

These two methods were applied to a scan volume from 17/6/2010 at Terrey Hills, which had substantial folding. Fig. 3.2 shows the raw scan of 3.1° elevation, the scan dealiasied with the 4DD method, and the scan dealiasied with the Tabary method. The Tabary method can be completed with some spatial (sweep) dealiasing identical to that used for the 4DD method. This is essentially a continuity check/enforcement, and will usually resolve undealiased or erroneous pixels, unless the bad data are isolated. Both methods effectively dealias the scan. If the rain is less contiguous, such as in isolated showers, neither method will perform well. For example, the Tabary method works best with data distributed around the radar.

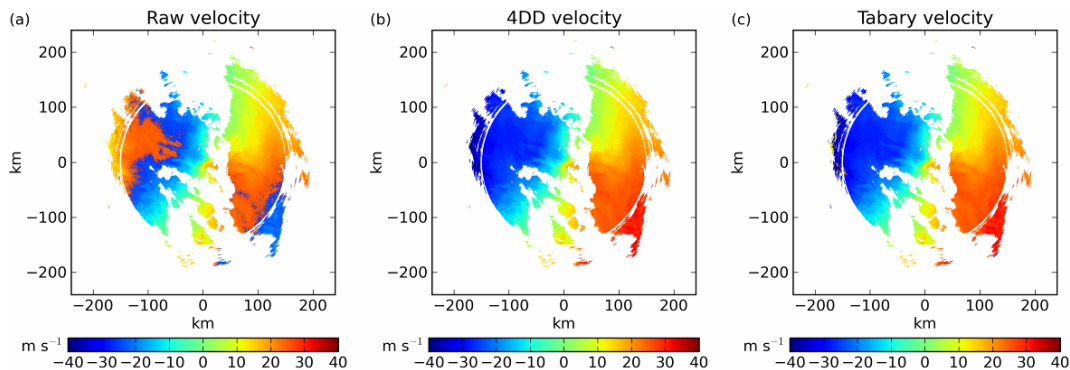


**Fig. 3.2** Data from Terrey Hills, 0200 UTC 17/6/2010 at 3.1° elevation. a) Raw radial velocity. b) Velocity dealiasied with 4DD method. c) Velocity dealiasied with Tabary method and no spatial dealiasing.

These methods both provide a fair degree of accurate dealiasing. However, dealiasing errors can occur, especially in areas with isolated or discontinuous rainfall, or noisy values. Ultimately, the 4DD method should be more accurate and faster to run, when applied to consecutive volumes. This algorithm has been adopted into future operational software.

A third dealiasing option is to use model wind to provide a basis for comparison. This could be done by taking the most-recently-available and highest-resolution forecast from NWP output. The radial wind may be interpolated from the model meridional and zonal winds, or extrapolated from a single profile at the radar location. Such a method is relatively fast and easy. However, it also relies upon an external source of information, which may not always be available in real time. There is a small chance that the model wind will severely disagree in direction with the observed wind, causing erroneous dealiasing. However, differences between model and observation of twice the Nyquist velocity are likely to be unusual in instances where strong winds are driven by large-scale systems, which are generally well-represented by the model. Ultimately, this method is most likely to be applied at the stage of assimilating radial wind observations.

Dealiasing will be form part of the post-processing quality control software being developed at present. The dealiased velocity, along with the raw data and other QC information, will be stored in hdf5 format following the OPERA Data Information Model standard. For all downstream radial velocity applications, the dealiased velocity should be used.

### **3.3 Data quality issues**

Various issues that may affect data quality can be dealt with during post-processing. These issues are primarily associated with non-weather echo. For example, ground and sea clutter need to be removed if inadequately filtered during on-site processing. Clear air echo should be identified and may be used or excluded from wind estimation, as discussed in Section 4. This section deals primarily with the errors in velocity estimates caused by data quality problems. Development of methods to remove clutter is dealt with elsewhere (Peter *et al.*, submitted).

Permanent ground clutter particularly affects radars situated in or near hilly regions. Ground echo is exacerbated in conditions where atmospheric refraction causes the radar beam to propagate nearer than normal to the ground. This anaprop causes non-permanent ground or sea clutter echoes to appear, and is particularly common for radars near the coast. In the Doppler signal ground clutter (from stationary targets) appears as a region of near-zero velocity, which collocates with high reflectivity. Ground clutter causes a low speed bias, and will also affect the observed wind direction. Sea clutter may have non-zero velocity, which makes it more difficult to detect and filter.

Current on-site radar processing attempts to remove ground clutter by analysing the raw signal, and filtering low-velocity signatures. This is occasionally ineffective and clutter signal remains. An example of this is shown in Fig. 3.3 and Fig. 3.4. These data are from 1200 UTC 28/9/2010 at Brisbane (Mt Stapylton). There were scattered showers (high reflectivity) and clear air echo (low reflectivity) about the radar. The clear air echo in this example has a weak and noisy signal. The ground clutter in the 1.3° elevation shows higher reflectivity (>0 dB) in Fig. 3.3 collocated with near-zero velocity in Fig. 3.4, while at the 0.9° elevation, the clutter is filtered. The effect on the velocity estimate can be demonstrated by calculating the VAD speed for each

elevation (Fig. 3.5). The clutter-contaminated speed estimate is approximately  $2 \text{ m s}^{-1}$  slower. Sea clutter causes similar problems: the velocity is typically nearer to zero, and the reflectivity is high.

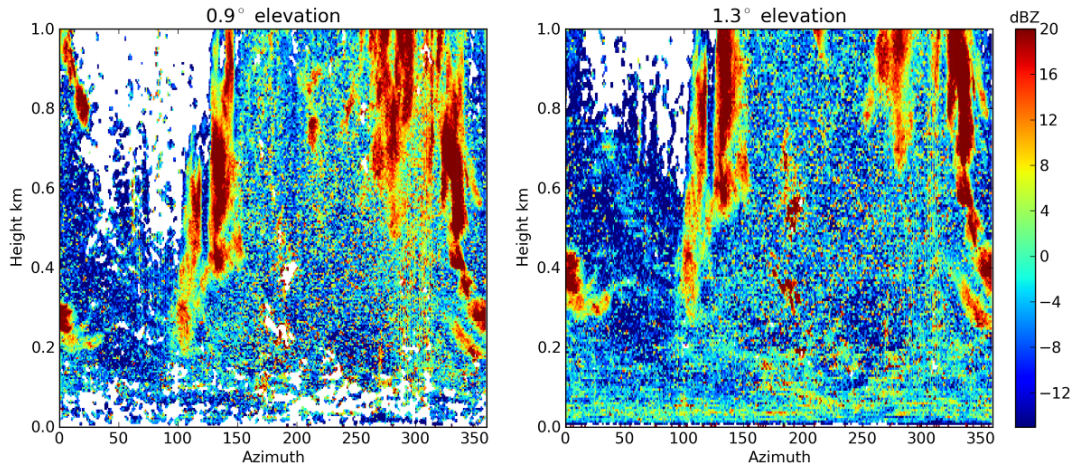


**Fig. 3.3** Reflectivity from 12 UTC 28/9/2010 at Brisbane (Mt Stapylton), for the 2<sup>nd</sup> and 3<sup>rd</sup> elevations. The clutter filtering was only effective on the lowest two elevations, producing the no-data areas (white) near the bottom of the left panel. The right panel instead shows reflectivity above zero. The height is calculated using equation 1.

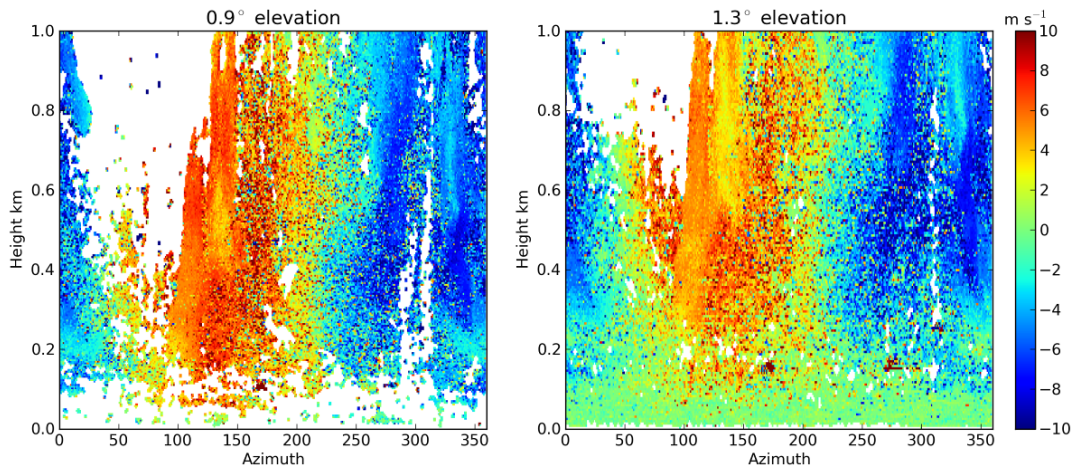


**Fig. 3.4** Velocity as for Fig. 3.3. The clutter in the right panel manifests as near-zero velocity at low altitude.

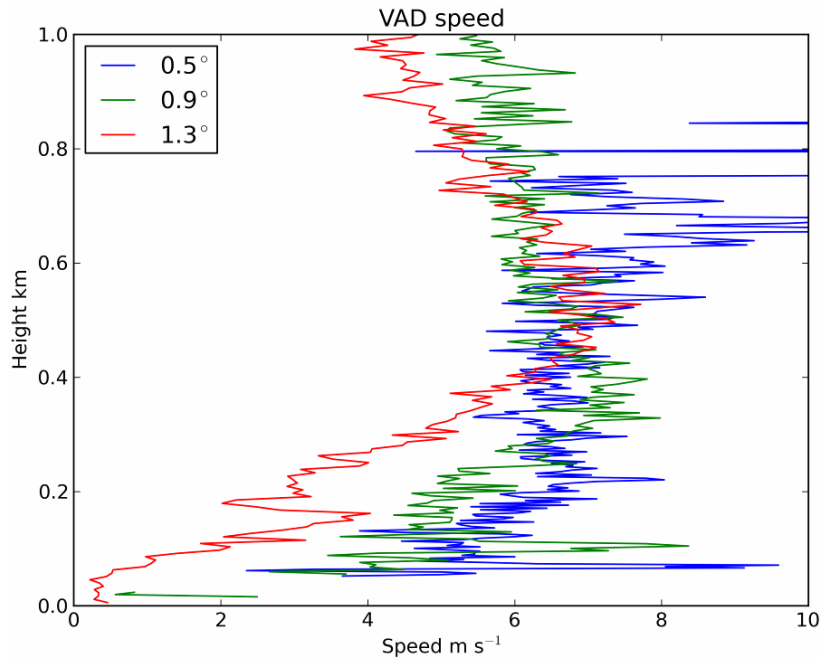


**Fig. 3.5 VAD speed for lowest three elevations from 12 UTC 28/9/2010 at Brisbane (Mt Stapylton). The near-ground speed is lower for the 1.3° elevation with ground clutter.**

Noisy signal is another problem that can affect velocity estimation, and so produce random variations in the velocity field. While spatial averaging (e.g. superobbing or VAD) reduces the effect of noisy data, it will still induce biases and errors. The noisiness can also cause erroneous dealiasing. Signal with high spatial variability can result from a high uncertainty in the measurement if it is near the signal-to-noise threshold, or if the spectral width is high. There are thresholds applied to both of these parameters in on-site processing, which limits this problem for post-processing. Signal variability can also result from non-weather targets moving with independent velocity. This can include insects, birds, bats and planes.

Occlusion, where the beam is partly blocked by the ground, can also cause biases. Completely obstructed beams cause problems for reflectivity measurements because there is no distinction between 'no signal' and 'no precipitation'. This is a lesser concern for velocity. However, partly blocked beams can cause a bias in the velocity measurement. The beam only illuminates a fraction of a normal volume, and so the velocity estimate will be derived only from scatterers in that part of the volume. This is typically the upper part of the volume, and the bias will be worse at low elevations. There may therefore be discrepancies between the occluded velocity estimate and that of adjacent, non-occluded beams.

The above issues may have varying degrees of negative impact on downstream applications. Ground clutter and sea clutter, the most common and problematic contaminants, will be removed using post-processing quality control. Weak or noisy signal may also be handled with thresholds, target identification, etc. There are no plans yet for handling occluded beams. A statistical treatment comparing with model winds may show if there is a bias that can be related to occlusion.

## 4. CLEAR AIR ECHO

Clear air echo can be returned from airborne insects, birds and bats (aerofauna), chaff from aeroplanes, and smoke from bushfires. Bushfires are common in the dry months in Australia, and occasionally are devastating to the inhabitants. However, these events are relatively isolated and usually of short duration. Chaff likewise appears sporadically, and lasts a few hours. Aerofauna are commonly seen during the warmer months, usually when undertaking migration or dispersion at high altitude. Clear air echo from insects may be present day or night, can extend to 50–100 km range on a good day, and 1–2 km in altitude. Reflectivity of up to 10–30 dB has been observed; such strong clear air echoes are difficult to separate from precipitation echoes. Bird and bat echoes are mostly observed at sunrise or sunset.

There has been increasing interest in making use of clear air echo from weather radar, including an increasing number of related presentations at recent radar meteorology conferences such as ERAD or the American Meteorological Society's Conference on Radar Meteorology. Weather services in various countries are considering the use of insect velocity observations as a proxy for wind estimation (e.g. Rennie *et al.*, 2010; Rennie *et al.*, 2011a). Such an application can provide a substantial increase in the temporal and spatial coverage of radar wind observations; however the observation bias can be prohibitive since large insects can fly at several  $\text{m s}^{-1}$ . Given the availability of insect echo in Australia, it is worthwhile to consider how useful such observations could be for NWP. To this end a quantification of uncertainty and bias is required.

Radar can also provide useful information on aeroecology (Frick *et al.*, 2010), i.e. insect or bird migration (although major bird migrations are few in Australia). Applications include tracking the migration of agricultural pests to provide early warning (e.g. Leskinen *et al.*, 2011). Migration involves a long-distance displacement conducted seasonally between different breeding grounds and feeding grounds, and in response to changing weather (Farrow and Drake, 1991; Drake, 1994; Dingle and Drake, 2007; Chapman and Drake, 2010). Long distance migration is done at substantially higher altitudes than foraging travel, occurring at hundreds of metres above ground level, where the wind speed largely controls the displacement. The migration height is thermally restricted; fauna that heat their bodies (e.g. birds, some large insects) can tolerate colder temperatures (Drake and Farrow, 1988). Observation by the author during the course of a year indicates abundant clear air echo during the spring and summer months (Sept–Mar). There is less clear air echo in winter, even in the north where it isn't cold. Insect numbers may be controlled also by food availability during the northern dry season.

### 4.1 Insects

Most radar entomological work in Australia has been conducted on macrolepidoptera (moths), particularly *noctuidae* and *sphingidae*, and locusts (*acrididae*—grasshoppers), such as *Chortoicetes terminifera* (Australian plague locust). Other types of migrating or dispersing insects would be present, including smaller insects, aphids, mosquitoes and flies, ballooning spiders, etc. However, the very small insects are unlikely to be detected by C- or S-band radar.

Locusts inhabit inland agricultural areas such as central-western NSW, the domain of the plague locust. The other Australian locusts, the spur-throated locust and the migratory locust, are primarily located in northern areas, particularly Queensland (Fig. 4.1). Locust distribution

mostly coincides with areas where there is no radar coverage. Where they do migrate within radar range, the observed radial velocity should be treated carefully. Grasshoppers can achieve airspeeds of several  $\text{m s}^{-1}$  (10 ft/s) (Clark 1969), which may introduce a serious bias for Doppler measurements with clear air. Plague and spur-throated locusts typically take off at dusk to migrate, although airborne numbers usually drop away by midnight (Drake and Farrow, 1983). The locust population can vary greatly in size, depending in part on the preceding weather conditions; plague years occur sporadically, usually when there are wet years to build the population (Walton *et al.*, 2003). Spring and summer of 2010–2011 was a major locust plague season. There were widespread locust reports in Queensland, New South Wales and Victoria, and parts of South Australia (Australian Plague Locust Commission (APLC) website). Locust migrations were observed by radar in some remote inland areas, although generally the reported locust sightings as compiled by the APLC were outside coverage range. Localised swarming (near-ground travelling and feeding) is too low to be detected by radars; only long-distance nocturnal migrations can be observed with weather radar.

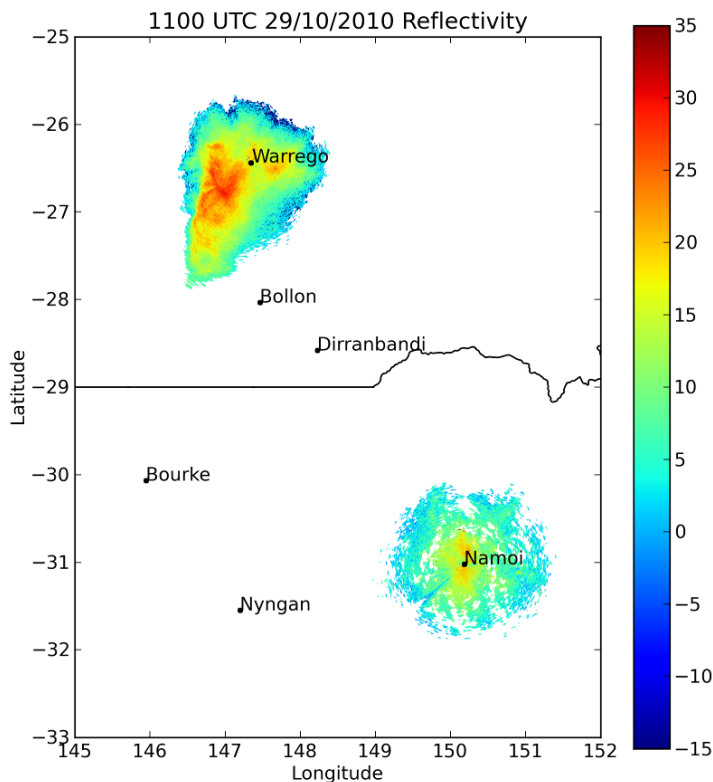


**Fig. 4.1** Locust migration (unidentified species) in south-east Queensland and northern NSW in October 2010. The asymmetric reflectivity at Warrego denotes a distinct patch of locusts that migrated southwestward. Around Namoi the insects are more uniformly distributed. (Data holes due to ground clutter.)

Noctuid moths, the other large night-flying insect type (besides *acrididae*), are well studied in south-eastern Australia. Commonly observed species include *Hippotion scrofa*, *Agrotis infusa*, *Persectania ewingii*, *Heliiothis punctigera*, *Mythimna convecta* and *Agrotis munda*, (Drake *et al.*, 1981; Gregg *et al.*, 1993). They have been found migrating as far as Tasmania in spring (Drake *et al.*, 1981), when warm NNW winds carry them great distances. Studies using light traps in northern NSW have provided surveys of nocturnal migrants. It was found that the more

numerous moth catches were associated with weather patterns that favour migration: windy rather than calm periods (Gregg *et al.*, 1993). Unsettled convective weather also favours migration (Farrow and Drake, 1991). Although not investigated, it may be assumed that moths make up a substantial portion of nocturnal migrants, and would constitute the majority prior to the start of locust migration.

There are also many diurnal migrants visible with the radars (Fig. 4.2), of which there is little information in published literature. Most radar entomology studies have focused on nocturnal insects, as these are observed more clearly (A. Drake, pers. comm. April 2011). Diurnal migrants are usually seen during warm, convective weather. They are supposed to include small insects that use convective updrafts to ascend, and need warmer temperatures. These are aggregated into convective cells or line structures where the air converges, as in Fig. 4.2.

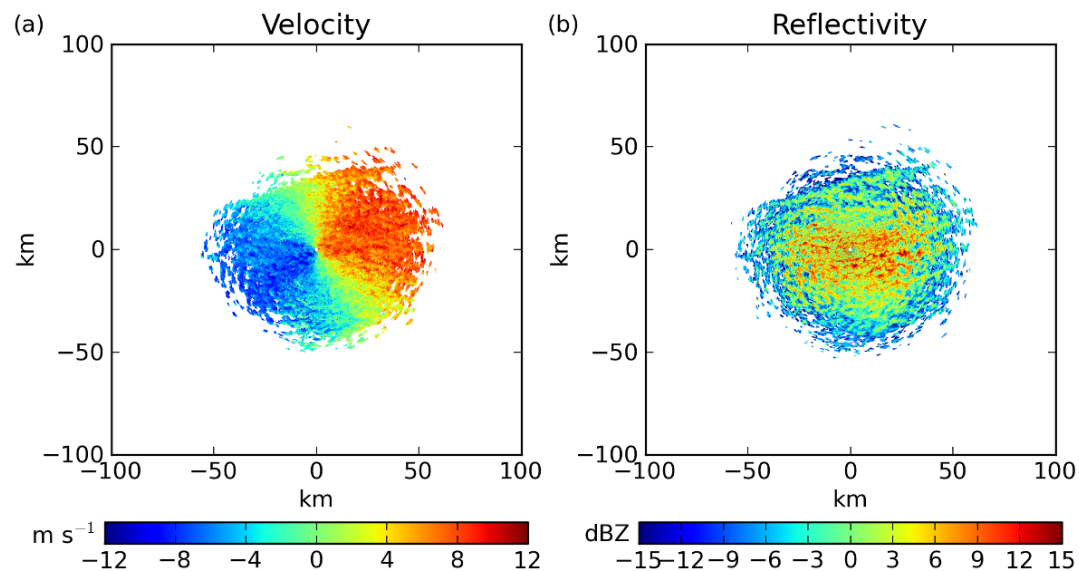


**Fig. 4.2** Diurnal migration on the afternoon of 30/12/2010, at Yarrowonga, featuring insects aggregated by convergence lines around convective cells.

A substantial study of insect migration was made with the Yarrowonga radar, prompted by the observation of ‘common orientation’ during the summer of 2010/11 (Rennie, accepted for publication). Common orientation implies that insects are directing their migration to travel to a more favourable habitat, or to maximise their distance travelled by heading downwind (e.g. Chapman *et al.*, 2010; Reynolds *et al.*, 2010). This study allowed the opportunity to look for evidence of insect bias arising from active insect migration.

Common orientation is revealed through a symmetric dumbbell shape appearing in the reflectivity. This results from oblate targets in alignment producing a larger reflected signal when illuminated side-on than head-on or tail-on (Fig. 4.3). When compared with the velocity from the Doppler measurement, the ambiguity of the orientation can be resolved by assuming the insects are not carried against the prevailing flow direction. Applying the VAD technique, the difference between the orientation and direction of travel can be measured as a vertical profile at the radar location. For example, Fig. 4.4 shows an instance of common orientation in the morning, with insects aggregated in the residual nocturnal inversion and jet. The insects were travelling north-eastward, but facing northward. Detecting common orientation using

reflectivity requires a fairly uniform horizontal distribution of targets. During the season studied, this did not often occur at night due to a high frequency of unsettled weather, and sometimes due to the initial ground density of insects (Rennie, accepted for publication).

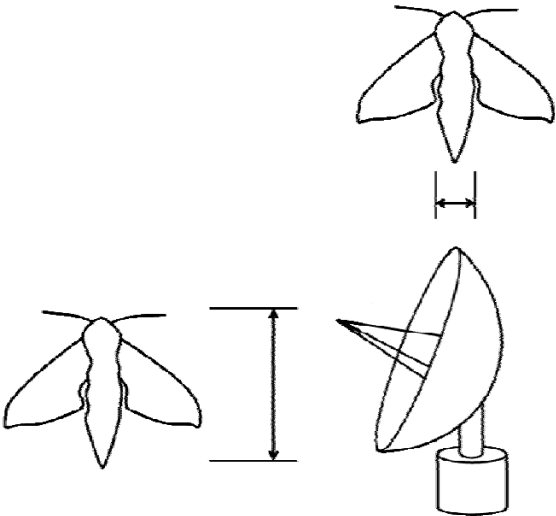


**Fig. 4.3** Schematic showing that insects present a larger target to the radar when illuminated side-on than head-on.

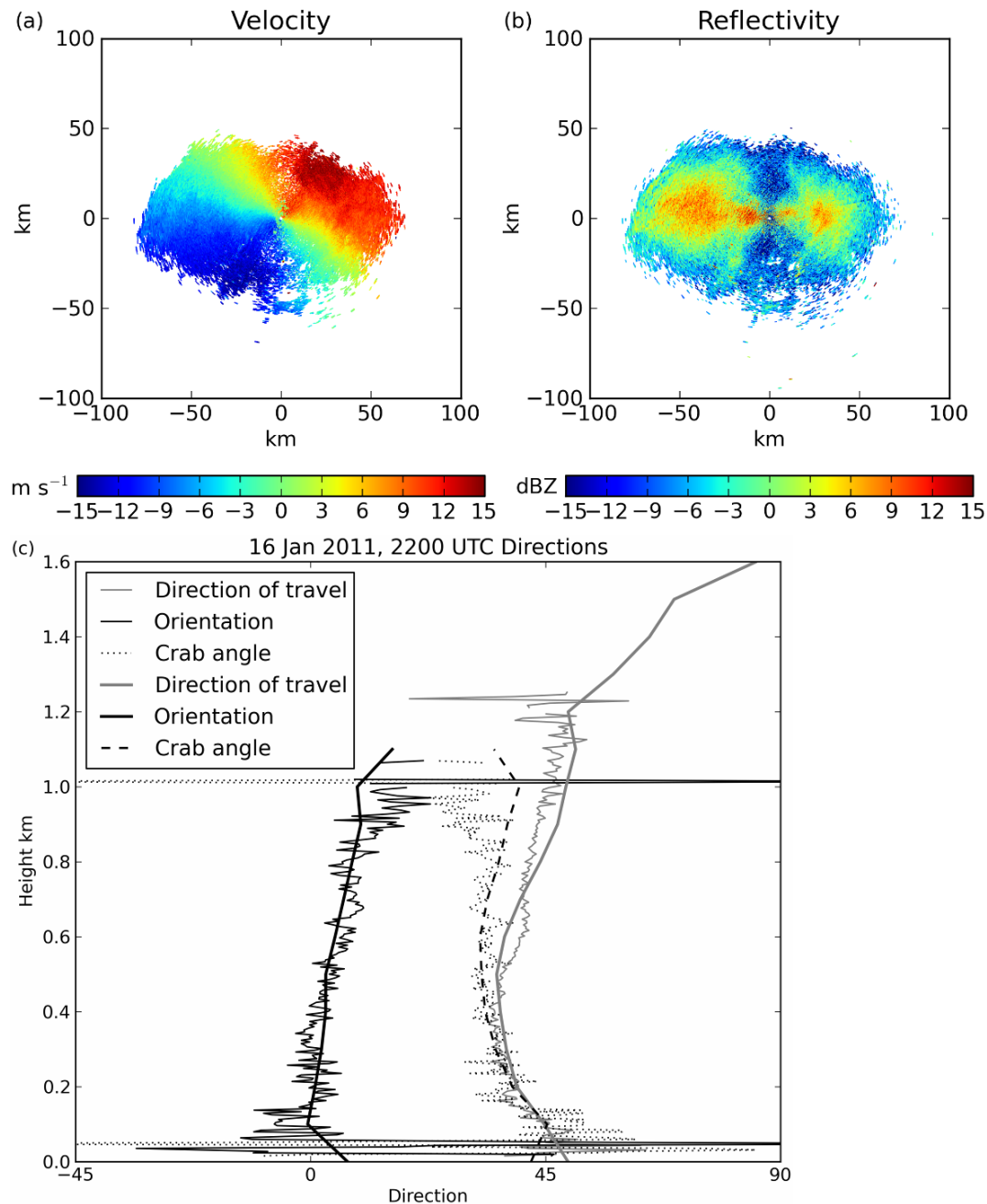


**Fig. 4.4** Example of common orientation in an early morning migration. a) Velocity of insects (blue towards radar). b) Reflectivity showing dumbbell with lobes to east and west of radar. c) Vertical profiles of the direction of orientation, direction of travel and crab angle (difference). Thick lines are volume-averaged, thin lines are for the  $0.9^\circ$  scan. Directions are given in degrees clockwise from north.

When observable, the insect orientation frequently differed from the direction of travel by more than  $30^\circ$ . More detail is given in Rennie (accepted for publication). This suggests that the insects were strongly attempting to control their migration. However, comparison with surface wind and model wind profiles indicated very little difference between the radar-derived velocities and these independent velocities. Although the surface wind observations are separated in height

from the radar measurement by tens of metres, there was consistently overlap with the observed direction of travel at the lowest levels of the radar scan.

#### 4.1.1 Comparison with model velocities

Model velocity profiles provided the most collocated basis for comparison, and therefore may be used to estimate biases in the insect-derived velocity. Fields from operational ACCESS-A (~12 km) analyses and forecasts of up to 5 hours were used. The column of model horizontal velocity data nearest to the Yarrowonga radar location was extracted. This required first interpolating meridional and zonal wind fields to the theta (temperature) grid, since the model uses a staggered (Arakawa C) grid whereby not all variables are on the same grid.

The differences between model and radar velocities were calculated by first interpolating VADs from radar data volumes to model levels up to 3 km above sea level. Data from all date-times and heights were analysed jointly. 17 cases between late October 2010 and February 2011 were used in the study, and in some cases two times from one case were used in the model comparison. More detail can be found in Rennie (accepted for publication). The differences in speed and direction were typically in the order of  $<2 \text{ m s}^{-1}$  and  $<30^\circ$  (Fig. 4.5), with mean values very near zero. Such values are within reasonable observation uncertainties for quantitative NWP applications. The mean speed difference was  $0.3 \text{ m s}^{-1}$  and RMS difference was  $2.1 \text{ m s}^{-1}$ . The distribution of speed differences was positively skewed, with a mode falling between  $-1$  and  $-2 \text{ m s}^{-1}$  (Fig. 4.6). The largest discrepancies occurred when there was a nocturnal jet for which the model height and observed height differed. The mean and RMS

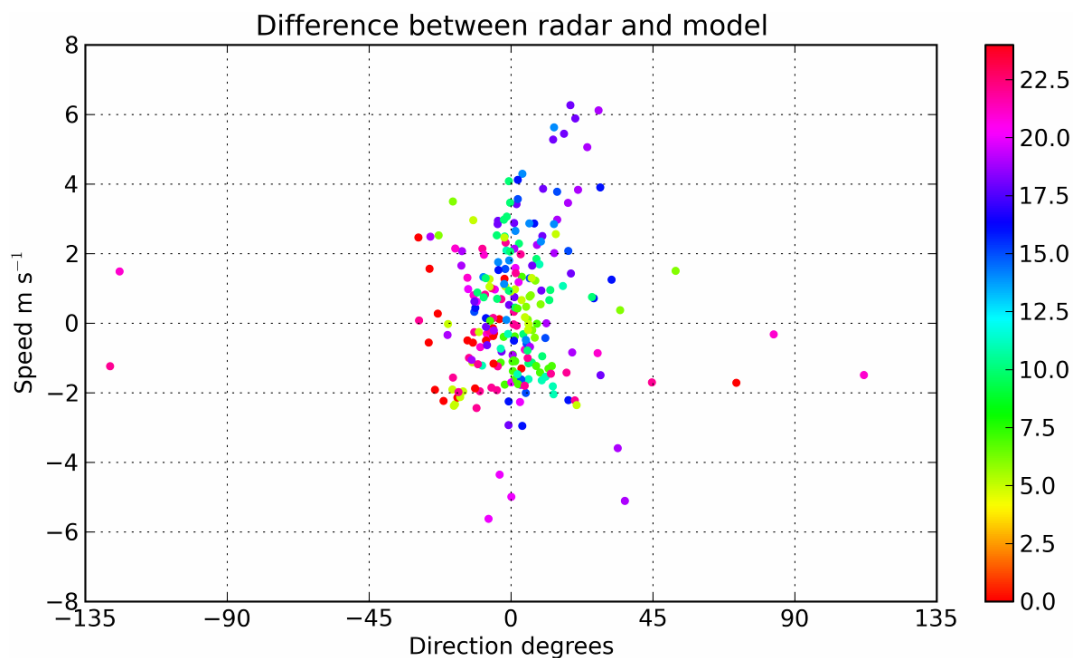


**Fig. 4.5 Comparison of clear air VADs with ACCESS-A model profile values (observation – background) of speed and direction. Data are coloured according to time of day in hours (UTC). Each data point represents a date-time and height.**

direction differences were  $2^\circ$  and  $22^\circ$  respectively. Overall, it was concluded that usually the effect of insects migrating with non-zero airspeed is either fairly small or not persistent.

However, a much larger data set would be necessary for a statistical analysis to properly characterise biases.

A similar analysis was made for insect echo from Emerald. There are a few differences between the two data sets. Firstly, the Emerald radar is S-band not C-band. Secondly, the wind velocity was typically observed to be low, often less than  $5 \text{ m s}^{-1}$ . Finally, little sign was seen of common orientation. This may be partly due to the low wind speeds, but was also due to non-uniform insect distribution. The effect of insect speed might be expected to be more obvious in this case.

For the analogous analysis using Emerald data, eleven instances were used, although eight were from two consecutive days, at 6-hourly intervals. This data set is half the size of that for Yarrowonga. The mean speed and direction biases were  $-0.5 \text{ m s}^{-1}$  and  $14^\circ$ , with RMS values of  $2.2 \text{ m s}^{-1}$  and  $59^\circ$  respectively. The speed difference showed a small negative skewness, in contrast with that of Yarrowonga, and the insect speeds were on average slower than the model velocity. The modal speed difference was however similar for both radar sites. Much of this speed bias distribution was due to the near ground ( $<700 \text{ m}$ ) velocities, where the insect speed was consistently lower. This could be contributed to by clutter contamination or model bias.

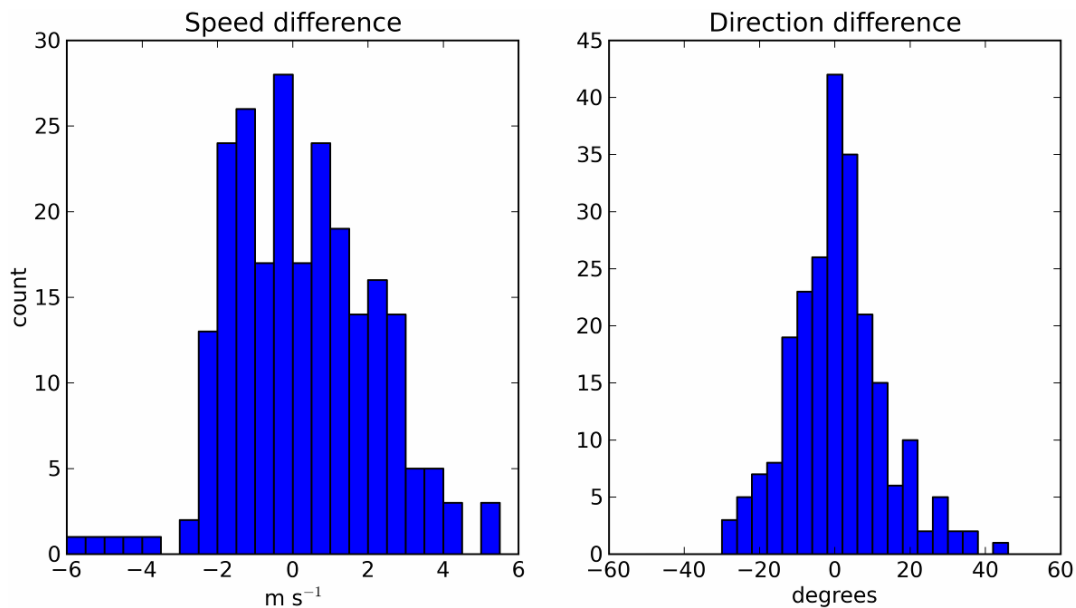


**Fig. 4.6 Histogram of speed differences (left) and direction differences (right) (observation – background). The direction outliers have been excluded. Cumulative counts are from 22 instances and all available heights, as per Fig. 4.5.**

The effect of insect airspeed on the observed velocity is considered in Table 4.1. Values in this table were derived by vector calculation in the horizontal plane. A range of likely insect air speeds were considered. For example, assuming an insect air speed of  $4 \text{ m s}^{-1}$ , at  $30^\circ$  to the wind direction, the radar observation may overestimate the wind speed by 13%, and the direction bias to around  $20^\circ$ . Provided that the insect speed is small, these biases are within the scope of observational error for applications like data assimilation. In conditions with very low wind speeds, e.g.  $2 \text{ m s}^{-1}$ , it would be wiser to exclude clear air echo.

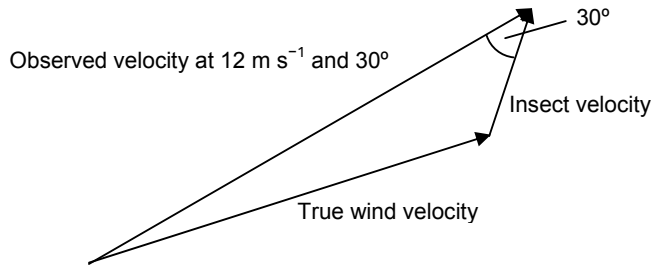


**Fig. 4.7** Schematic of velocity vectors used for Table 4.1, where the Observed vector remains constant, and the length of insect air speed varies.

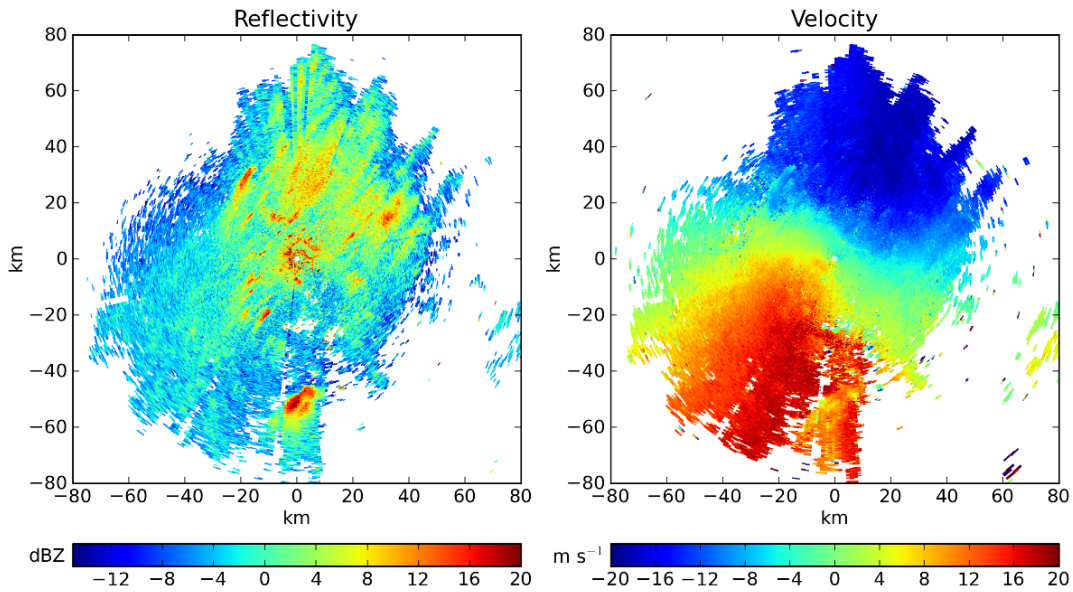
**Table 4.1** True wind speed assuming insects have air velocity in the direction of their orientation, and at various speeds, assuming the observed velocity (ground speed) is 12 m s<sup>-1</sup> and 30°.

Insect air speed m s <sup>-1</sup>	True wind speed m s <sup>-1</sup>	True wind direction
0	12	30.0°
2.0	11.14	21.05°
4.0	10.58	10.89°
6.0	10.39	0.0°

## 4.2 Bird migration and dispersal

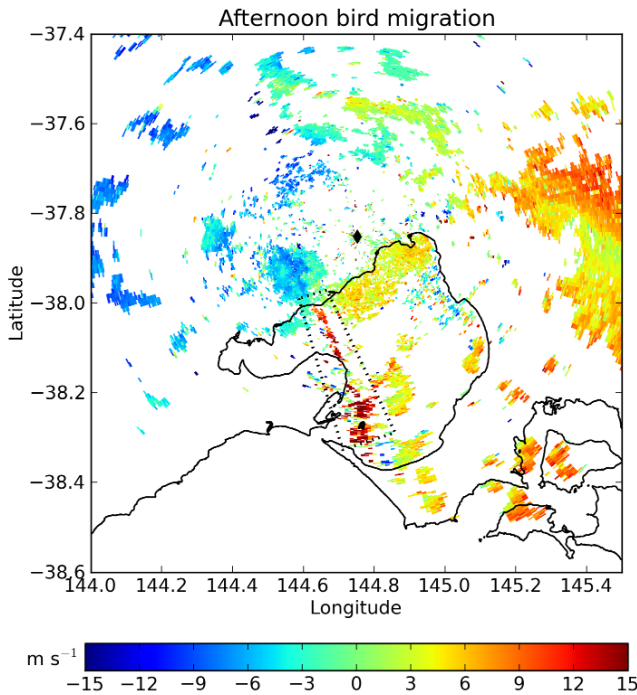
Bird migration can have a large effect on the retrieved velocity, since birds are large targets that can fly quickly. Most occurrences of birds observed by radar in Australia are during migration or dispersal between feeding and roosting areas, which may be short trips in both distance and duration. Australia has few major bird migrations like those seen in other parts of the world.

Fig. 4.8 shows a dawn dispersal of birds from overnight roosts: backscatter targets emerging from point locations. These are probably waterbirds living near the river located just north of the Yarrowonga radar. There are some variations in the velocity field as a result of the birds. This dispersal pattern lasted less than half an hour. Shortly after this, dawn insects also take off for migration. Water bird numbers also wax and wane over various years. Due to recent wet years, waterbird numbers have increased greatly in 2011 (ABC News, 2011).



**Fig. 4.8 Dawn bird dispersal, at 0432 EST, 6/1/2011 at Yarrowonga. The points of high reflectivity indicate birds taking off and travelling south-southwestward.**

Fig. 4.9 shows an afternoon migration of birds across Port Phillip Bay in Melbourne. These produce a velocity signal which is at odds with the local wind velocity as indicated by nearby precipitation echo. This kind of echo is brief and isolated, but may be difficult to detect automatically.



**Fig. 4.9 Radial velocity at 0.5° elevation marking the bird migration across Port Phillip Bay in the afternoon at 1524 EST 15/9/2011, observed from the Melbourne radar. The radar location is marked by ♦; the bird migration is enclosed with the dashed box. The migration appears as a line of red velocity value as the birds travel south-southeastward.**

### 4.3 Fire observations

Bushfires, though infrequent, have a high impact, so very rapid and accurate forecasts are required to advise authorities and prevent loss of life. Large fires can have a local effect on the weather, such as producing pyrocumulus clouds that would not be reproduced in a NWP model. Doppler radar observations from fires can provide additional wind information at high resolution. In the first instance the smoke can indicate the location of the fire. The radar can also provide information about the plume behaviour, with high horizontal resolution, although vertical resolution may be coarser, depending on range.

An example from the devastating 2009 Black Saturday (7/2/2009) bushfires near Kinglake and Marysville, east-northeast of Melbourne, is shown in Fig. 4.10. Unfortunately in this case the radar experienced technical problems due to the excessive heat of the day (up to 48 °C), and ceased operation in between the times shown in Fig. 4.10. The smoke was clearly drifting with the wind and dispersing slowly, after emanating from a localised fire early in the day. Later in the day, the wind had shifted from northwest to southwest, and the swath of smoke shows a more complex wind field, which arose from a large burning area.

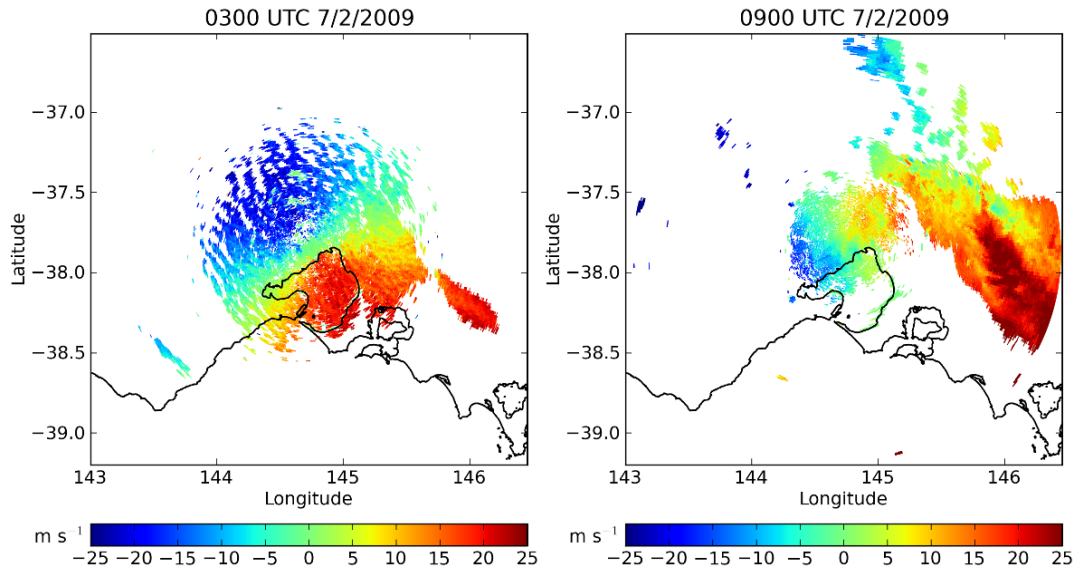


**Fig. 4.10** Velocity from 2009 Black Saturday bushfires, 2/7/2009. At 0300 UTC there are two main fires, though one is obscured by clear air. At 0900 UTC, around sunset so minimal clear air, smoke from the bushfire complex is visible. There are also some scattered showers.

### 4.4 Chaff

Chaff is metallic material released by military aircraft, with the intention of masking the plane from radar detection. In Australia it is occasionally released during airforce exercises, and appears in weather radar scans. This echo type is sporadic and may be difficult to identify automatically. Chaff may make a useful wind tracer as it disperses, but would interfere with radar QPE. Chaff has its own initial velocity when ejected from the aircraft so may not, at least initially, represent the wind velocity. An example of chaff is shown in Fig. 4.11. It is identifiable as a narrow linear or angular trail that advects with the wind and disperses or falls out typically within hours.

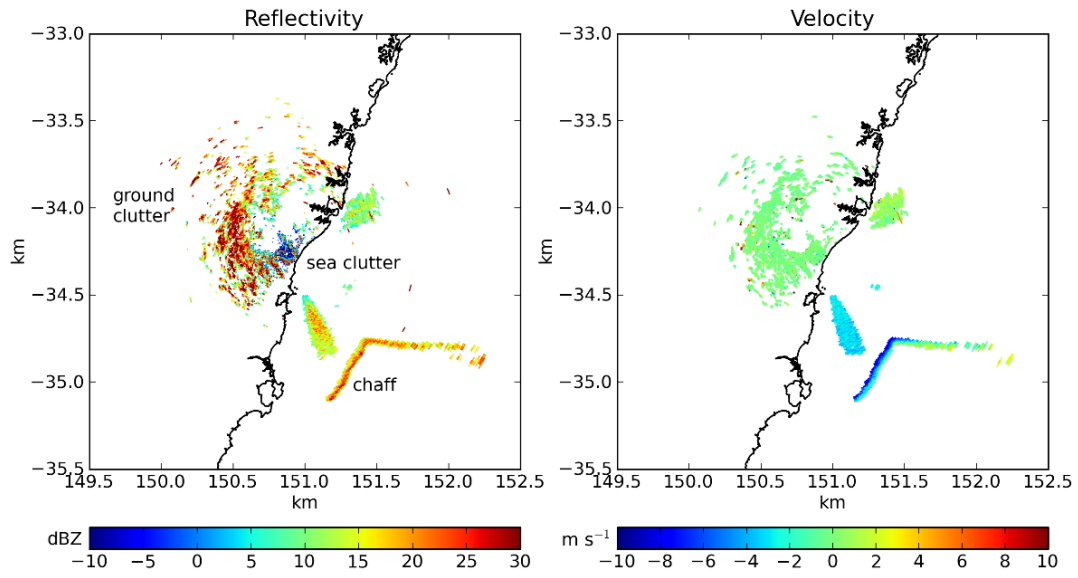


**Fig. 4.11** Ground and sea clutter and chaff viewed with Wollongong radar (0.5° elevation scan) on 17/10/2011 at 0500 UTC.

## 5. WEATHER FEATURES OBSERVED WITH DOPPLER RADAR

Weather radar provides high spatial and temporal resolution observations of a range of weather features in the troposphere. Examples include small-scale wind features, distribution and propagation of showers, atmospheric waves and convergence lines. Doppler radar gives further information on the atmospheric motion associated with these features. In this section examples of various weather features detectable by Doppler radar are discussed.

The following example is of atmospheric waves, possibly Kelvin-Helmholtz waves, viewed at the Yarrowonga radar (Fig. 5.1). Such waves have been observed with dual Doppler and polarimetric radar in the United States (Houser and Bluestein, 2011). At Yarrowonga, waves with wavelength on the kilometre scale (gravity waves or solitary waves) have been observed propagating across the radar scan area, preceding or sometimes following precipitation, i.e. a storm outflow or gust front. Such features were common on nights with insect migrations, when the weather was unsettled. Most often a solitary wave was observed, but occasionally a train of several waves emerged and then dissipated before leaving the region of the radar observation. These types of waves have a relatively short lifespan, and that they are so often observed with this radar suggests they occur frequently in this region of Australia. As discussed in Section 4.1, insect migration often coincides with unsettled weather; hence storm outflow is similarly common at these times. Insect echo is particularly useful to facilitate observation of such waves. The example in Fig. 5.1 did not result in a substantial change in the wind field, although some cause a large change in speed or direction.

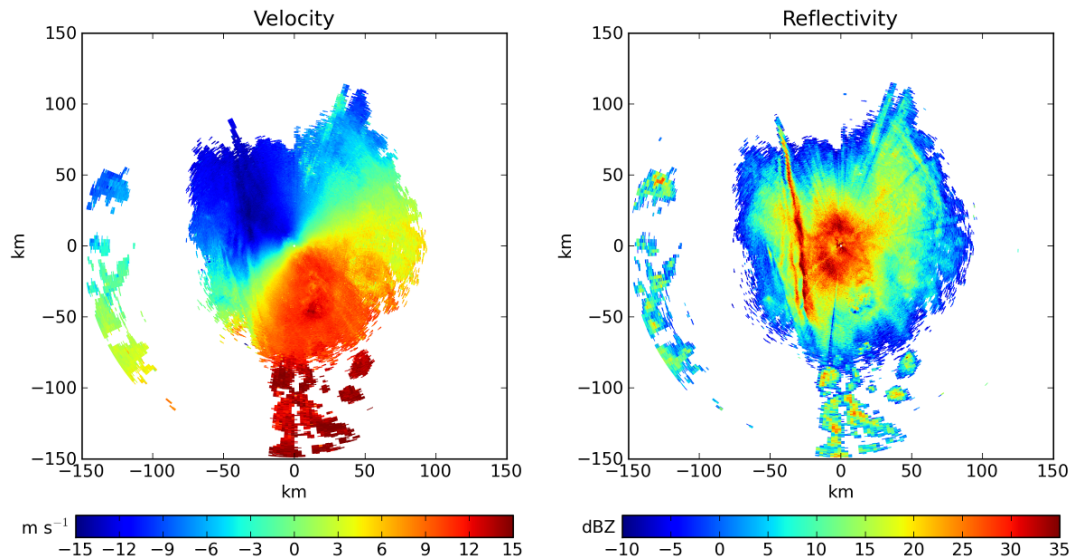


**Fig. 5.1 Velocity (left) and reflectivity (right) scans taken by the Yarrowonga radar from 1412 UTC 24/11/2010. Rain approaching from the west is preceded by a boundary that formed a wave train propagating west to east. Three lines are visible in the reflectivity.**

Sea breeze fronts are similarly visible with radar, particularly where there is strong clear air echo. These are similar in appearance to gust fronts seen inland, with a reflectivity line marking the boundary of a wind change. Sea breezes, however, are the result of the contrast between land and sea after diurnal heating, so are seen to propagate inland from the coast, usually during

the afternoon. Fig. 5.2 shows several sea breeze fronts travelling north, with curvature mimicking the shape of the coastline where they formed. In this particular example a cold front was approaching from the west, and the associated wind front, travelling eastward, arrived in Melbourne shortly before the sea breeze. As the sea breeze propagated inland, it bowed this cold front feature locally northward (Fig. 5.2a) until the two merged into one single boundary, although the western part remained distinct (Fig. 5.2b). In this case there was a substantial change in the wind field after the front passed.

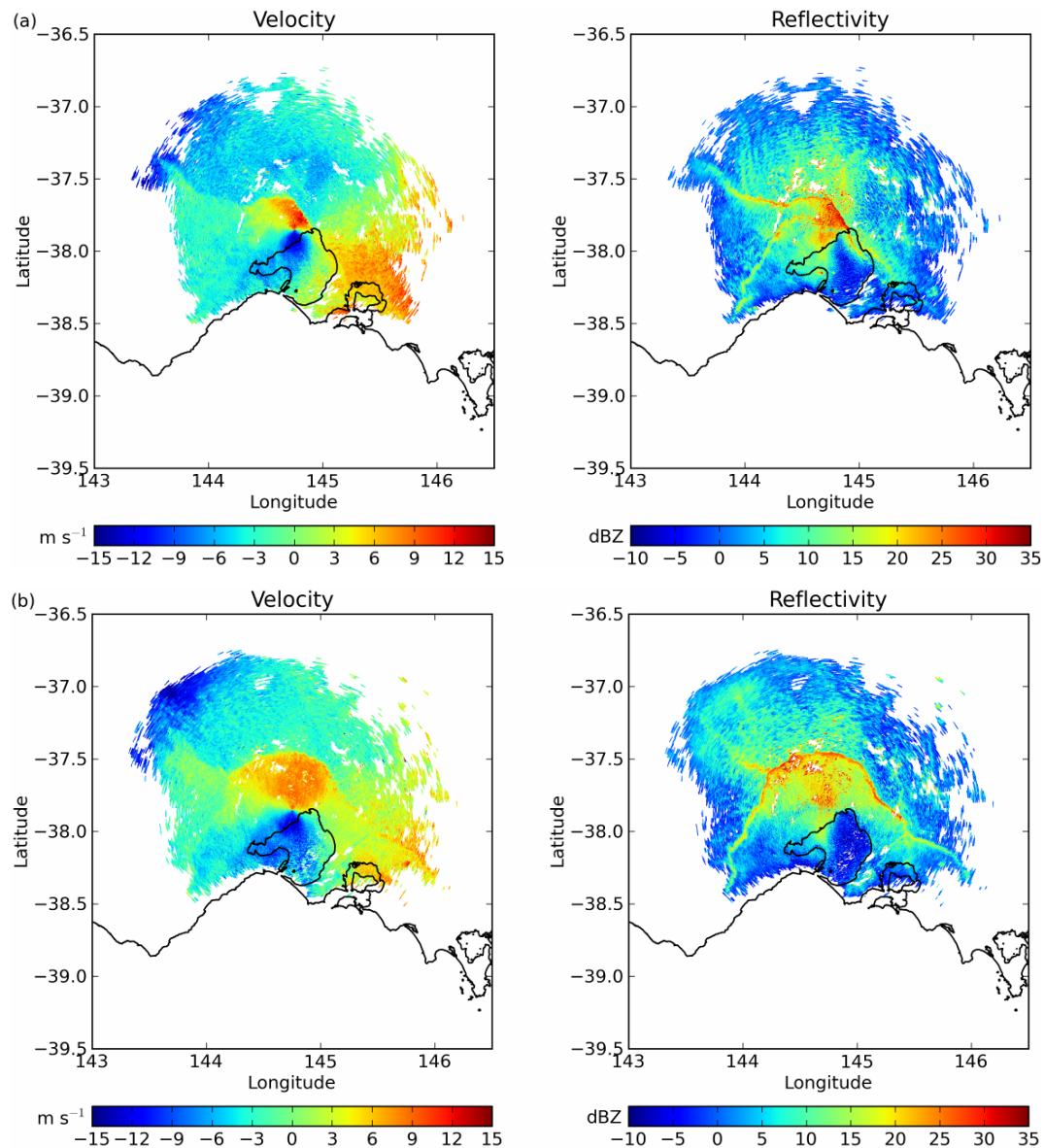


**Fig. 5.2** Velocity and reflectivity scans at 0.9° elevation, from the Melbourne radar. a) 0236 UTC 21/1/2011. A cool change moving in from the west is closely followed by a sea breeze passage from the south. b) 0348 UTC 21/1/2011. The front and sea breeze have merged north of Port Phillip Bay, but a second sea breeze front has developed to the east, from the Western Port Bay inlet to the east of Port Phillip Bay.

Tornadoes large enough to be detected at the radar resolution appear in Doppler radar scans as a dipole in the velocity field. The following example (Fig. 5.3) from near Adelaide was reported crossing near Port Noarlunga (ABC News, 2009). There are few enough tornadoes in Australia that examples within Doppler radar coverage and close enough to the radar location to be resolved are rare. When there is a tornado-related signal in the radial velocity, it appears as a (red and blue) dipole denoting the cyclonic shear.

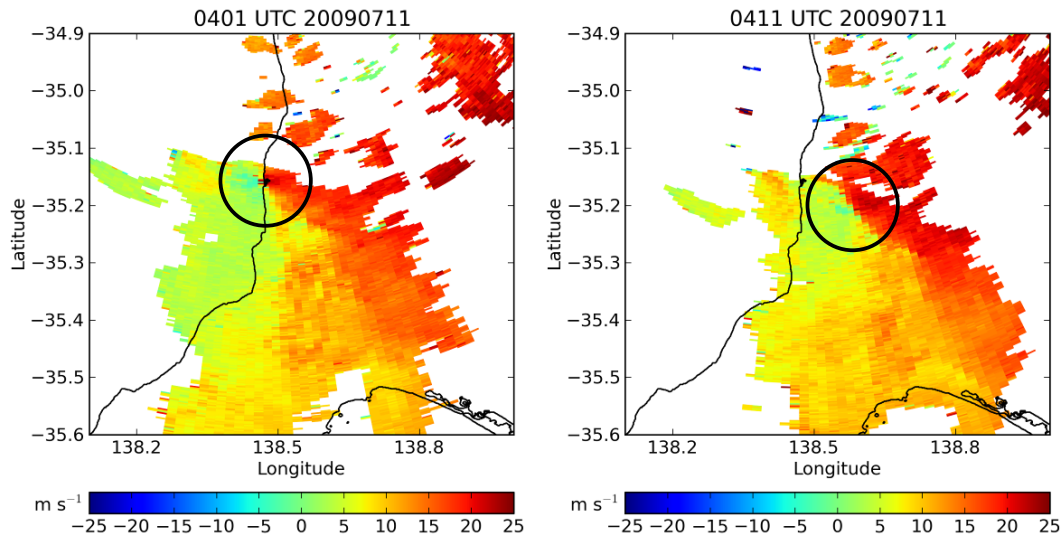


**Fig. 5.3 Tornado passage during a storm passing south of Adelaide. Scans are 0.5° elevation from Buckland Park radar at 0401 and 0411 UTC 11/7/2009. The Buckland Park radar is just north of the upper axis limit. The tornado is circled. It is inferred by the dipole in the velocity field.**

Radar can provide observations of large-scale storms, including tropical cyclones. The radar fields can show the structure and movement of the tropical cyclone. Normally tropical cyclones form over the tropical sea, not over land-based radars. Strong tropical cyclones passing directly over radars, such as tropical cyclone Yasi over the Willis Island radar in 2011, are likely to damage the instruments. A recent example of a well-observed tropical cyclone is Carlos, which formed over Darwin (Fig. 5.4). This rare example can provide some insight into the storm development process, as well as quantifying vortex parameters (V. Kumar, pers. comm.). As the centre of rotation is near the radar, and the rotation covers a large area, the velocity field alone does not show the clear dipole like the tornado example. The rotation can be inferred from the asymmetry of the wind field, i.e. the maximum and minimum radial velocity are not diametrically opposite with respect to the radar, but shifted toward the cyclone eye. When the eye of TC Carlos passed very close to the radar, the radial velocity dropped towards zero, as the wind velocity became largely tangential to the radar beam.

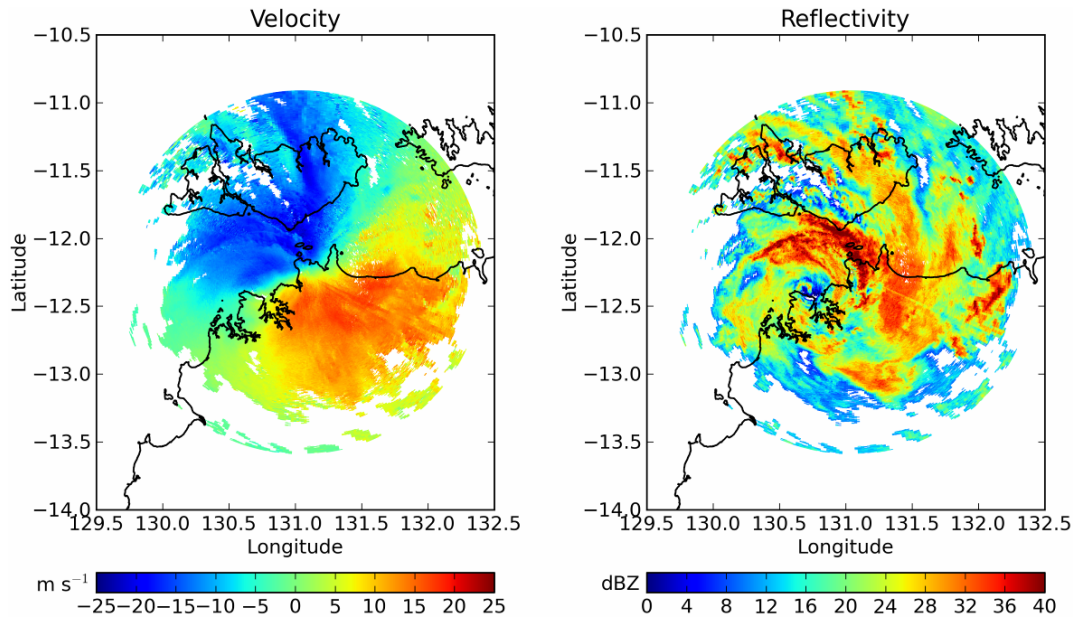


**Fig. 5.4 Velocity and reflectivity from TC Carlos, Darwin (Gunn Pt research radar) at 2200 UTC 15/2/2011.**

As shown in the above examples, radar can visualise weather on scales ranging from a few kilometres to tens of kilometres. Radar observations of weather features that are able to be resolved by numerical models will be able to inform the initial conditions for NWP by providing detail on this scale. Finer scale features would not be resolved by the model, and may not be resolved by the superobservations that are actually assimilated. This information is therefore lost from data assimilation. For example, the waves in Fig. 5.1, with a scale of around 5 km, would not be reproduced by the model analysis with 1.5 km horizontal grid spacing, but the sea breeze and associated wind change featured in Fig. 5.2 should be resolved.

## 6. COMPARISON AGAINST OTHER OBSERVATIONS

### 6.1 Comparison with a wind profiler

Within Australia's sparse observation network, there are few Doppler radars located near wind profilers. Some profilers are used in a research capacity so data are not always reliable or available. The Terrey Hills radar is near a wind profiler (WP) at Sydney Airport, 25 km to the south, that runs operationally. This was the best choice for a comparison. The study is detailed in Rennie *et al.* (2011b).

These two Sydney instruments were compared for 11 days with various weather conditions. The radial winds were converted to a vertical profile using the VAD method described in Section 3.1. VADs from all elevations in a volume were averaged in 100 m height intervals. It is important to remember that the wind profiler measures the velocity directly above it, whereas the radar measures the velocity at some distance from the instrument and from this infers the velocity at the instrument location. Therefore the wind estimate may be poor when the wind field is non-linear across the Sydney Basin. For this study, no range limit was applied to VAD calculations, although estimates with high uncertainty in the least-squares fit were excluded. VAD values at high altitude would have a larger error. The available heights at any time varied according to the weather, but the maximum was around 9 km altitude.

Generally the two instruments' observations compared well. Combined statistics were calculated for all profiles and all heights available. The RMS difference in speed was  $3.6 \text{ m s}^{-1}$  and RMS difference in direction was  $37^\circ$ . The WP had previously been demonstrated to have a slow bias in comparison with a collocated radiosonde (Vincent *et al.*, 1998). Here a slow bias was similarly found, the WP profiles being on average  $1 \text{ m s}^{-1}$  slower than the VADs. The direction was also expected to be less accurate at low speeds for both instruments, and this was reflected in the poorer agreement at low speed ( $<4 \text{ m s}^{-1}$ ). The vector correlation for different velocity ranges is shown in Table 6.1.

**Table 6.1** Vector correlation coefficient ( $r^2$ ) (Crosby *et al.*, 1993) between VAD and WP data separated by WP speed, and number of samples (n). (Reproduced from Rennie *et al.* (2011b))

Data range	$r^2$	n
All data	0.79	9399
$>8 \text{ m s}^{-1}$	0.82	4517
$4\text{--}8 \text{ m s}^{-1}$	0.62	3379
$<4 \text{ m s}^{-1}$	0.29	1503

There was no substantial difference in bias for when VADs were derived from precipitation or clear air echo, although the larger discrepancies at low speeds would include any contribution from non-zero insect air speed. It is advisable to avoid clear air echo when the speed is comparable to the likely insect air speed. Finally, the typical differences between the WP and

insect VADs were comparable to those of insect velocities with model velocity profiles, shown in Fig. 4.5. Therefore using radial wind from clear air without introducing large errors may be possible.

## 6.2 Comparison with Automatic Weather Stations

Comparison of the radar-measured radial velocities with ground-based wind observations is not trivial. The radars measure a high altitude (tens to hundreds of metres a.g.l. at the lowest elevation) and a large volume, whereas Automatic Weather Stations (AWS) provide near-surface point observations. Radial wind components can't be compared directly with the wind velocity at the AWS location because the radial velocity is effectively a scalar quantity, whereas the AWS measure a vector quantity. Comparison by converting the AWS wind vector to an equivalent radial velocity does not prove useful because discrepancies could be due to either speed or direction. Instead a comparison of the lowest part of the VAD wind profiles was made with nearby AWS wind measurements. The VAD is a vector velocity averaged over an area but intended to represent the radar location. The AWS data were recorded at one minute intervals and were then subsampled to 10 minute intervals. This analysis entails a comparison of observations representing different heights and different horizontal resolutions. However, given the scarcity of observations with which to make comparisons, this analysis has some value. It at least demonstrates the degree of comparability between the observation types.

The first example is from 9/12/2010, a day that provided one of the cases in the insect orientation study (Rennie, accepted for publication) summarized in Section 4. Data are from the Yarrawonga region, which is an inland region with fairly flat terrain, during fair weather conditions with only clear air echo. The four AWS were within 70 km of the radar. There was fair agreement in speed and direction (Fig. 6.1), including a change in direction when a wind front passed during the night (at ~1300 UTC). However, the AWS showed more high-frequency variation with time than the VAD. There was an expected increase in speed with height, both between the ground stations and the VAD, and among the different VAD heights. This was noticeable particularly when the speed aloft increased. Note that part of this vertical wind speed gradient may be influenced by ground clutter contamination at low levels. During the daytime the speed gradient was less than during the night (after the front passed). There was also a systematic difference in direction with height. The lower level winds were generally more positive than winds aloft. This conforms to the Ekman spiral configuration, where surface winds are deflected to the right of winds aloft.

The second example is taken from a coastal location—Sydney (Terrey Hills)—which has greater variations in terrain than Yarrawonga. Spatial variations in the velocity field, such as the sea breeze, result in poor VAD estimates due to non-linearity. In this example, 30/9/2010, a sea breeze passed shortly before 0200 UTC, and is apparent in Fig. 6.2 via an increase in speed, and convergence of AWS directions at this time. There was strong vertical shear during the night-time, with very weak surface winds, but stronger winds aloft. During some periods there was a more positive wind direction near the surface, indicating Ekman spiralling. However, the shear manifested mostly as a variation of speed not direction with height, particularly at night.

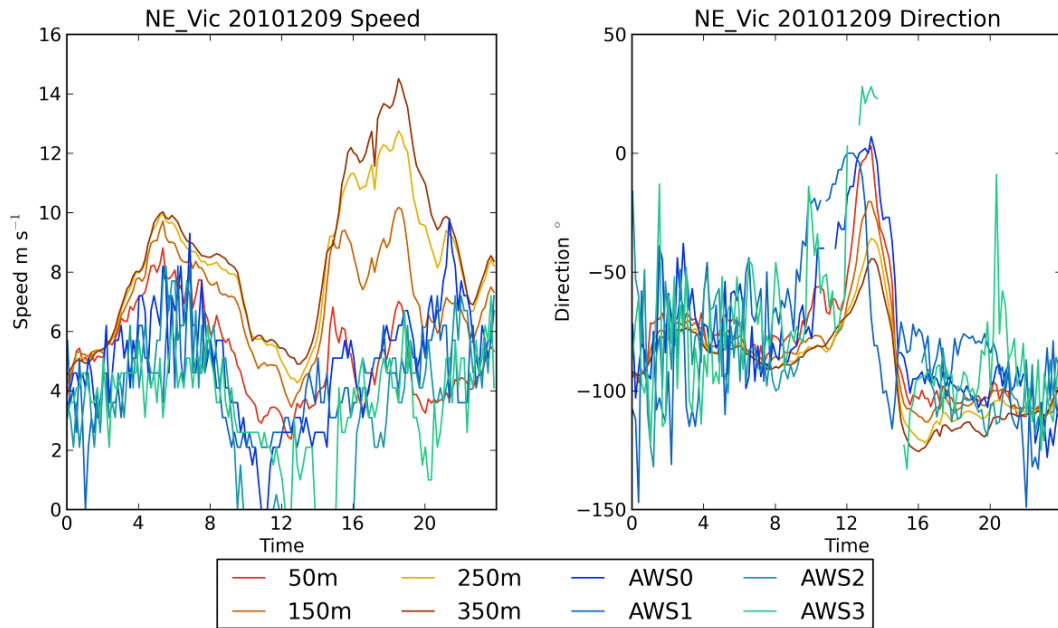


**Fig. 6.1** Comparison of Yarrowonga VAD with subsampled 1 minute AWS wind observations. Speed (left) and Direction (right) are shown. VAD heights are relative to antenna height and represent the middle of the 100 m height bin. AWS stations are Yarrowonga, Shepparton AP, Rutherglen and Wangaratta Aero. Time is in UTC.

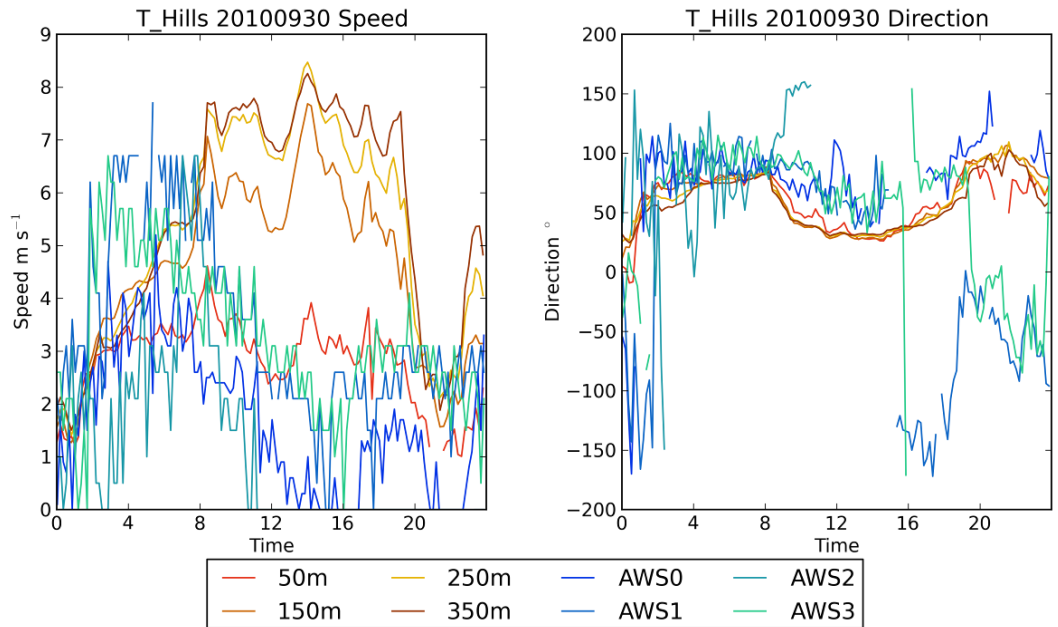


**Fig. 6.2** Comparison of Terrey Hills VAD with subsampled 1 minute AWS wind observations. Speed (left) and Direction (right) are shown. VAD heights are relative to antenna height and represent the middle of the 100 m height bin. The AWS stations are Sydney AP, Kurnell, Terrey Hills and Richmond RAAF. Time is in UTC.

The conclusions that can be drawn from the above examples are that there are periods when there is reasonable agreement between surface observations and observations above ground level, considering the sources. Discrepancies due to shear are particularly obvious in the speed differences. Therefore, while radar observations can provide some indication of near-surface velocities, they cannot substitute for surface observations. Similarly, surface observations may not give an accurate indication of conditions aloft, with accuracy much reduced more than a few tens of metres above ground level.

## 7. ASSIMILATION OF RADIAL WINDS

Assimilation of radar data requires a model with comparable horizontal grid resolution, i.e. in the order of a few kilometres or less. In the first instance the Bureau of Meteorology will apply assimilation to high-resolution city domains with  $\sim 1.5$  km horizontal grid resolution. These model domains are situated around the capital cities, most of which have Doppler radars in the vicinity. The domains are typically  $6^\circ$  by  $6^\circ$  (approximately 600 km by 600 km), and may contain observations from one to four Doppler radars.

The potential volume that the radar covers is a wedge of a dome of radius indicated in Table 2.1, dependent upon the backscatter coverage in the volume. However, only a limited selection of raw data would be ingested for assimilation. The limits imposed on the raw data are due to the density and uncertainty in the observations. For assimilation, it is desirable to have an observation density not greater than the model grid resolution. Near the radar the observation resolution is much greater than model grid resolution. Densely-located observations with correlations could bias the analysis. It is also difficult to minimize the cost function to resolve the analysis with large numbers of dense observations (D. Simonin, pers. comm., 2009). Limiting the observation usage to those with low uncertainties (e.g. in location) also helps reduce observation density and better informs the analysis.

The radars all scan over a large number of elevations, typically 14, as listed in Section 2. Not all of these would be used for assimilation. The lower elevation radar beams overlap, so these should be avoided as both redundant and highly correlated. For example, using elevations of  $0.9^\circ$ ,  $2.4^\circ$ ,  $4.2^\circ$  and  $5.6^\circ$  would avoid overlapping beams. The lowest elevation scan is excluded as having the most problems with clutter and occlusion. The higher elevations are also excluded: they have a greater error due to the greater contribution of the vertical component of the radar targets' velocity (the vertical component is not assimilated at present). At  $5.6^\circ$  the velocity will contain a 0.5% contribution from vertical velocity. In stratiform rain this gives the impression of convergence towards the radar. Additionally, the high elevation beams may quickly pass above the weather and so provide little information. However, sometimes a correction is applied for the vertical component of the beam trajectory, and a vertical (fall) velocity for rain can be estimated.

At long ranges, the uncertainty in the beam's vertical position will increase, particularly for low elevations. This is because atmospheric refraction causes the beam to bend, as described in Section 2.1. In a standard atmosphere the beam bends away from the surface more slowly than is accounted for by the Earth's curvature. However, the beam path varies with the atmospheric refractivity, particularly at low elevations. For example, in some circumstances the beam is bent back to the earth's surface, producing an anaprop. Furthermore, the beam broadness means that the height at which the observation is representative is not known exactly; there may be precipitation in only part of the beam. Accounting for the beam trajectory and broadening produces small improvements, but not significantly better than a relatively simple observation operator (Järvinen et al, 2008). However, taking into account where in the beam the velocity is represented (due to reflectivity gradients and beam shape) will reduce bias and correlation errors (Fabry and Kilambi, 2011). Considering the results indicated by Fabry (2010), the data should therefore be truncated at 100–120 km range, beyond which the error in vertical position may be

substantial. The resulting potential spatial coverage with currently-installed radars, using a 120 km limit, is shown in Fig. 7.1.

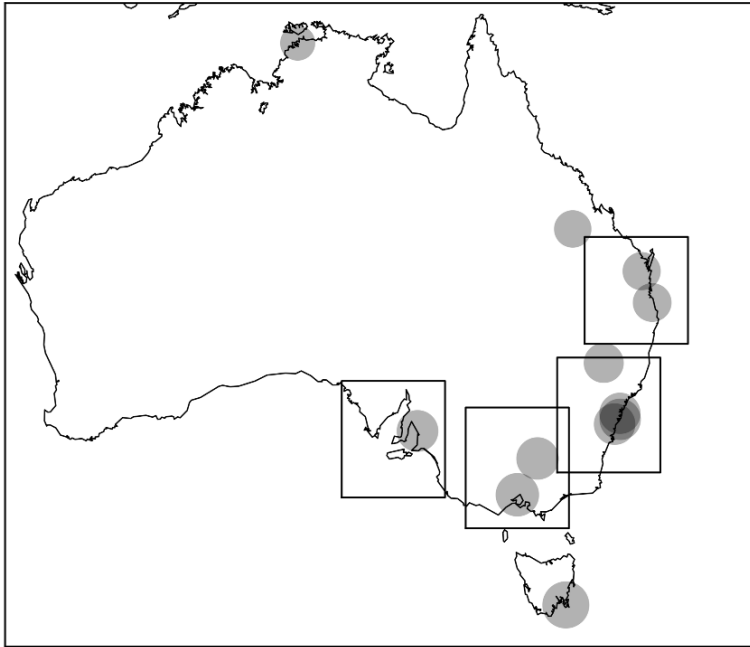


**Fig. 7.1 Potential radar coverage to 120 km (shaded), and approximate city domains for the 1.5 km ACCESS high resolution model.**

Assimilation of radial winds has a few requirements. Firstly, that echoes only from precipitation (or e.g. insects if desired) can be accurately selected for use. Secondly, that an estimate of observation error can be produced, which may be dominated by the representativeness error; this is to say, the difference between how the radar observes, and how this is represented with the model. Thirdly, that the observations are superobbed and thinned to reduce density and correlations. Finally, the observation covariances need to be suitably represented to control the spread of information. The information in this report should be taken into consideration when preparing for assimilating radial velocity.

## 8. CONCLUSION

The Australian Bureau of Meteorology has recently implemented Doppler capability in key locations in its radar network. These instruments provide a new source of observations with many useful applications. Doppler radar provides high spatial and temporal resolution measurements of radial velocity (in addition to the base reflectivity), so can give better coverage than other types of instruments that measure wind velocity. This coverage depends upon the presence and distribution of precipitation or clear air targets.

Spatial 'wind' velocity observations provide visualisation of a variety of weather features, which may be of aid to forecasters. These observations also indicate the movement of aerofauna such as birds and insects. On one hand, these new data may be of use to biological studies. On the other hand, clear air echo from insects can also be used to visualise weather features such as sea breezes and other boundaries when it is not raining.

Comparison of Doppler radar measurements with other velocity estimates was facilitated by creating VAD profiles. Generally the radar velocity profiles compared well with velocities from wind profiler data, AWS, and NWP model fields, indicating that the radar data give reasonable velocity estimates. The differences were typically of the order of a few  $\text{m s}^{-1}$ , which is indicative of the size of the uncertainty in the measurements. Although a bias from insect air speed is anticipated, this was not demonstrated to be substantial. The insect-derived velocities did not show a greater bias than precipitation-derived velocities: the VAD errors were generally comparable. The findings of this study do not exclude use of insects for wind estimate in Australia, although care should be taken, in particular at low wind speeds. Extensive monitoring by comparison with model radial velocities should further characterise the errors and biases.

For quantitative applications such as data assimilation, understanding the errors is important. Errors and correlations in the observations are reduced by superobbing and thinning. However, the uncertainty of the observation, and thus the weight given to the observation during assimilation, is dominated by the representativeness error. It should also be noted that the uncertainty in the vertical location of the radar beam increases with range, as does the height bias associated with inhomogeneity of backscatter targets in the sample volume. Beyond 100 km or so, this error may be significant, especially for low elevation scans. Therefore long-range observations should not be used for assimilation.

The intention for the future is to assimilate radial winds from precipitation, and optionally from clear air echo, into high resolution versions of ACCESS with city domains. This should improve the forecast of severe weather with lead times of 3 to 12 hours.

## **ACKNOWLEDGMENTS**

The author wishes to thank Jeff Keppert for helpful discussion about fire weather and Vickal Kumar for discussion about data for TC Carlos.

## REFERENCES

- ABC News. 2009. SA tornado hit speeds of 150kph. <http://www.abc.net.au/news/2009-07-12/sa-tornado-hit-speeds-of-150kph/1350310>. accessed: 18 Oct 2011.
- ABC News. 2011. Boom time for waterbirds across the Murray. <http://www.abc.net.au/news/2011-12-19/boom-time-for-water-birds/3737876>. accessed: 19 Dec 2011.
- Andersson, T. 1992. 'A method for estimating the wind profile and vertical speed of targets from a single Doppler radar.' In *WMO Technical conference on Instruments and Methods of Observation (TECO-92), Vienna, Austria*. World Meteorological Organization: Geneva.
- Australian Bureau of Meteorology. 'PC Based Rapid Transmitter Digital Receiver Option'. Weather Watch Radar Software Documentation, 94 pp.
- Bowler, N.E.H., Pierce, C.E. and Seed, A. 2004. Development of a precipitation nowcasting algorithm based upon optical flow techniques. *J. Hydrol.* **288**: 74-91.
- Browning, K.A. and Wexler, R. 1968. The determination of kinematic properties of a wind field using Doppler radar. *J. Appl. Meteorol.* **7**: 105-13.
- Chapman, J.W. and Drake, V.A. 2010. Insect Migration. *Enc. Anim. Behav.* **2**: 161-6.
- Chapman, J.W., Nesbit, R.L., Burgin, L.E., Reynolds, D.R., Smith, A.D., Middleton, D.R. and Hill, J.K. 2010. Flight orientation behaviors promote optimal migration trajectories in high-flying insects. *Science* **327**: 682-5.
- Crosby, D., Breaker, L. and Gemmill, W. 1993. A proposed definition for Vector Correlation in Geophysics: Theory and Application. *J. Atmos. Oceanic. Tech.* **10**: 355-67.
- Dance, S.L. 2004. Issues in high resolution limited area data assimilation for quantitative precipitation forecasting. *Physica D* **196**: 1-27.
- Dingle, H. and Drake, V.A. 2007. What is migration? *BioScience* **57**: 113-21.
- Doviak, R.J. and Zrnić, D.S. 1993. *Doppler Radar and Weather Observations*, Academic Press, Inc.: San Diego, CA.
- Drake, V.A., Helm, K.F., Readshaw, J.L. and Reid, D.G. 1981. Insect migration across Bass Strait during spring: a radar study. *Bull. Entomol. Res.* **71**: 449-466.
- Drake, V.A. and Farrow, R.A. 1983. The nocturnal migration of the Australian plague locust, *Chortoicetes terminifera* (Walker) (Orthoptera: Acrididae): quantitative radar observations of a series of northward flights. *Bull. Entomol. Res.* **73**: 567-85.
- Drake VA, Farrow RA. 1988. The influence of atmospheric structure and motions on insect migration. *Ann. Rev. Entomol.* **33**: 183-210.
- Drake, V.A. 1994. The influence of weather and climate on agriculturally important insects: An Australian perspective. *Aust. J. Agr. Res.* **45**: 487-509.

Dupuy, P., Matthews, S., Scovell, R.W., Kergomard, A., Bouyer, K., Huuskonen, A., Smith, A., Gaussiat, N. and Tabary, P. 2011. 'Odyssey: A European Radar Data Centre.' *35th Conference on Radar Meteorology, Pittsburg, PA*, American Meteorological Society.

Fabry, F. 2010. 'Radial velocity measurement simulations: common errors, approximations, or omissions and their impact on estimation accuracy.' In *ERAD 2010 - The Sixth European Conference on Radar in Meteorology and Hydrology, Sibiu, Romania, 6-10 September*.

Fabry, F. and Kilambi, A. 2011. 'The Devil is in the Details: Preparing Radar Information for its Proper Assimilation.' *35th Conference on Radar Meteorology, Pittsburg, PA, 25-30 September* American Meteorological Society.

Farrow, R.A. and Drake, V.A. 1991. *Migration*, Melbourne University Press: Carlton.

Frick, W.F., Chilson, P.B., Diehl, R.H., Howard, K.W., Kelly, T.A., Kelly, J.F., Westbrook, J.K. and Kunz, T.H. 2010. '*Advanced Radar Technologies for Studying Organisms in the Aerosphere*'. AIRE: Aeroecological Interdisciplinary Research and Education.

Ge, G., Gao, J., Brewster, K. and Xue, M. 2010. Impacts of beam broadening and Earth curvature on storm-scale 3D variational data assimilation of radial velocity with two Doppler radars. *J. Atmos. Oceanic. Tech.* **27**: 617-36.

Gregg, P.C., Fitt, G.P., Coombs, M. and Henderson, G.S. 1993. Migrating moths (*Lepidoptera*) collected in tower-mounted light-traps in northern New South Wales, Australia: species composition and seasonal abundance. *Bull. Entomol. Res.* **83**: 563-78.

Gunn, B., Jones, R., Lane, A., Morgan, E., Barnes, C., May, P.T. and Beyer, S. 2007. 'Operational configuration and software evaluation of the RNDSUP Doppler radars for the Australian weather radar network.' In *AMS 33rd Conference on Radar Meteorology, Cairns, Australia*. American Meteorological Society:

Hawkness-Smith, L.D., Charlton-Perez, C. and Ballard, S. 2011. 'Direct assimilation of radar reflectivity data in the Met Office convective scale forecast system.' *35th Conference on Radar Meteorology, Pittsburg, PA, 25-30 September* American Meteorological Society.

Houser, J.L., Bluestein, H.B. 2011. Polarimetric Doppler radar observations of Kelvin-Helmholtz waves in a winter storm. *J. Atmos. Sci.* **68**: 1676-702.

Hubbert, J.C., Dixon, M. and Ellis, S.M. 2009a. Weather radar ground clutter. Part II: Real-time identification and filtering. *J. Atmos. Oceanic. Tech.* **26**: 1181-97.

Hubbert, J.C., Dixon, M., Ellis, S.M. and Meymaris, G. 2009b. Weather radar ground clutter. Part I: Identification, modeling, and simulation. *J. Atmos. Oceanic. Tech.* **26**: 1165-80.

Huuskonen, A., Delobbe, L. and Urban, B. 2010. 'News on the European Weather Radar Network (OPERA).' *ERAD 2010 - The Sixth European Conference on Radar in Meteorology and Hydrology, Sibiu, Romania*. No. Advances in Radar Applications National Meteorological Administration.

James, C.N. and Houze Jr, R.A. 2001. A real-time four-dimensional Doppler dealiasing scheme. *J. Atmos. Oceanic. Tech.* **18**: 1674-83.

Leskinen, M., Markkula, I., Koistinen, J., Pylkkö, P., Ooperi, S., Siljamo, P., Ojanen, H., Raiskio, S. and Tiilikkala, K. 2011. Pest insect immigration warning by an atmospheric dispersion model, weather radars and traps. *J. Appl. Entomol.* **135**: 55-67.

Met Office. 2009. Radar. In (Ed, National Meteorological Library and Archive) Exeter.

Met Office. 2012. Weather Radar Network Renewal.

<http://www.metoffice.gov.uk/water/radarimprovements>, accessed: 10 Jan 2012.

Michelson, D., Szturc, J., Gill, R.S. and Peura, M. 2010. 'Community-based weather radar networking with BALTRAD.' *ERAD 2010 - The Sixth European Conference on Radar in Meteorology and Hydrology, Sibiu, Romania, 6-10 September*. No. Advances in Radar Applications National Meteorological Administration: Romania.

Michelson, D.B., Andersson, T., Koistinen, J., Collier, C.G., Riedl, J., Szturc, J., Gjertsen, U., Nielsen, A. and Overgaard, S. 2000. 'BALTEX Radar Data Centre Products and their Methodologies'. SMHI Reports. Meteorology and Climatology., Swedish Meteorological and Hydrological Institute: Norrköping.

Montmerle, T. and Faccani, C. 2009. Mesoscale assimilation of radial velocities from Doppler radars in a preoperational framework. *Mon. Wea. Rev.* **137**: 1939-53.

Mueller, C., Saxe, T., Roberts, R., Wilson, J., Betancourt, T., Dettling, S., Oien, N. and Yee, J. 2003. NCAR Auto-Nowcast System. *Weather Forecast.* **18**: 545-61.

Peter, J.R., Seed, A. and Steinle, P. submitted. A Bayesian methodology for detecting anomalous propagation in radar reflectivity images. *J. Appl. Meteorol. Clim.*

Rennie, S.J., Illingworth, A.J., Dance, S.L. and Ballard, S.P. 2010. The accuracy of Doppler radar wind retrievals using insects as targets. *Meteorol. Appl.* **17**: 419-32.

Rennie, S.J., Dance, S.L., Illingworth, A.J., Ballard, S. and Simonin, D. 2011a. 3D-Var assimilation of insect-derived Doppler radar radial winds in convective cases using a high resolution model. *Mon. Wea. Rev.* **139**: 1148-63.

Rennie, S.J., McIntosh, D., Steinle, P., Seed, A. and Tully, M. 2011b. A comparison between wind profiles from the Sydney (Terrey Hills) Doppler radar and the Sydney Airport wind profiler. *CAWCR Res. Lett.* **6**: 27-33.

Rennie, S.J. accepted for publication. Common orientation and layering of migrating insects in south-eastern Australia observed with a Doppler weather radar. *Meteorol. Appl.*

Reynolds, A.M., Reynolds D.R., Smith, A.D. and Chapman, J.W. 2010. A single wind-mediated mechanism explains high-altitude 'non-goal oriented' headings and layering of nocturnally migrating insects. *P. Roy. Soc. B-Biol. Sci.* **277**: 765-72.

Sugier, J., Parent du Châtelet, J., Roquain, P. and Smith, A. 2002. 'Detection and removal of clutter and anaprop in radar data using a statistical scheme based on echo fluctuation.' In *Proceedings of ERAD 2002 - The Second European Conference on Radar Meteorology, Delft, Netherlands, 18-22 November*.

Tabary, P., Scialom, G. and Germann, U. 2001. Real-time retrieval of the wind from aliased velocities measured by Doppler radars. *J. Atmos. Oceanic. Tech.* **18**: 875-82.

Vincent, R., Dullaway, S., MacKinnon, A., Reid, I., Zink, F., May, P.T. and Johnson, B. 1998. A VHF boundary layer radar: First results. *Radio Sci.* **33**: 845-60.

Walton, C., Hardwick, L. and Hanson, J. 2003. '*Locusts in Queensland*'. Pest Status Review Series - Land Protection, 45 pp., Department of Natural Resources and Mines, Qld: Brisbane.

Weber, M.E., Cho, J.Y.N., Herd, J.S., Flavin, J.M., Benner, W.E., Torok GS. 2007. The Next-Generation Multimission U.S. Surveillance Radar Network. *Bull. Amer. Meteor. Soc.* **88**: 1739-51.





The Centre for Australian Weather and  
Climate Research is a partnership between  
CSIRO and the Bureau of Meteorology.